High Arctic geopotential stress field and implications for geodynamic evolution

CHRISTIAN SCHIFFER[1]*, CHRISTIAN TEGNER[2], ANDREW J. SCHAEFFER[3], VICTORIA PEASE[4] & SØREN B. NIELSEN[2]

[1]*Department of Earth Sciences, Durham University, Durham DH1 3LE, UK*

[2]*Department of Geoscience, Centre of Earth System Petrology, Aarhus University, 8000 Aarhus, Denmark*

[3]*Department of Earth and Environmental Sciences, University of Ottawa, 120 University, Ottawa, Ontario, Canada, K1N 6N5*

[4]*Department of Geological Sciences, Stockholm University, Stockholm 106 91, Sweden*

**Correspondence: christian.schiffer@zoho.com*

Abstract: We use new models of crustal structure and the depth of the lithosphere–asthenosphere boundary to calculate the geopotential energy and its corresponding geopotential stress field for the High Arctic. Palaeostress indicators such as dykes and rifts of known age are used to compare the present day and palaeostress fields. When both stress fields coincide, a minimum age for the configuration of the lithospheric stress field may be defined. We identify three regions in which this is observed. In north Greenland and the eastern Amerasia Basin, the stress field is probably the same as that present during the Late Cretaceous. In western Siberia, the stress field is similar to that in the Triassic. The stress directions on the eastern Russian Arctic Shelf and the Amerasia Basin are similar to that in the Cretaceous. The persistent misfit of the present stress field and Early Cretaceous dyke swarms associated with the High Arctic Large Igneous Province indicates a short-lived transient change in the stress field at the time of dyke emplacement. Most Early Cretaceous rifts in the Amerasia Basin coincide with the stress field, suggesting that dyking and rifting were unrelated. We present new evidence for dykes and a graben structure of Early Cretaceous age on Bennett Island.

The lithospheric structure and surface geology in many regions of the Arctic remain poorly defined. Consequently, many aspects of the tectonic evolution of this remote area are a matter of significant debate. We discuss the Phanerozoic tectonic evolution of the Arctic by comparing palaeostress indicators, such as dykes and rifts, with an estimate of the present day stress field, the World Stress Map (WSM; Heidbach *et al.* 2010) and the calculated geopotential stress field. In the study area, the WSM is constructed almost entirely from earthquake focal mechanisms and borehole breakouts. Dyke swarms of Mesozoic and younger ages are distributed at various locations along the North American and Greenland Arctic margins, as well as the Barents Sea, Taimyr Peninsula and the New Siberian Islands. Large extensional rift systems of different ages are present along the Arctic shelves as well as onshore. We compute the lithosphere-derived present day stress field by calculating the geopotential stress field that results from lateral pressure differences in the lithosphere. The lithospheric density model used for calculating the geopotential energy (GPE) is a compilation of new data, including sedimentary thickness, crustal thickness, dynamic topography (Lebedeva-Ivanova *et al.* 2015, in review) and the lithosphere–asthenosphere boundary (LAB) (Schaeffer *et al.* in review; Schaeffer & Lebedev 2015*b*). A comparison of spatially overlapping structures of varying age with the present day stress field (WSM) allows the large-scale interpretation of the evolution of the stress field and insight into the tectonic evolution of the High Arctic.

Tectonic evolution

The tectonic evolution of the High Arctic is complex and a number of aspects remain incompletely understood, largely due to the lack of densely and homogeneously distributed geological and geophysical constraints. Although many components are a matter of significant debate, there are a number of major plate tectonic reconfigurations and tectonothermal events which are better understood and are briefly reviewed in the following. An overview of the geographical locations and major tectonic features is shown in Figure 1.

From: Pease, V. & Coakley, B. (eds) *Circum-Arctic Lithosphere Evolution*. Geological Society, London, Special Publications, **460**, https://doi.org/10.1144/SP460.6

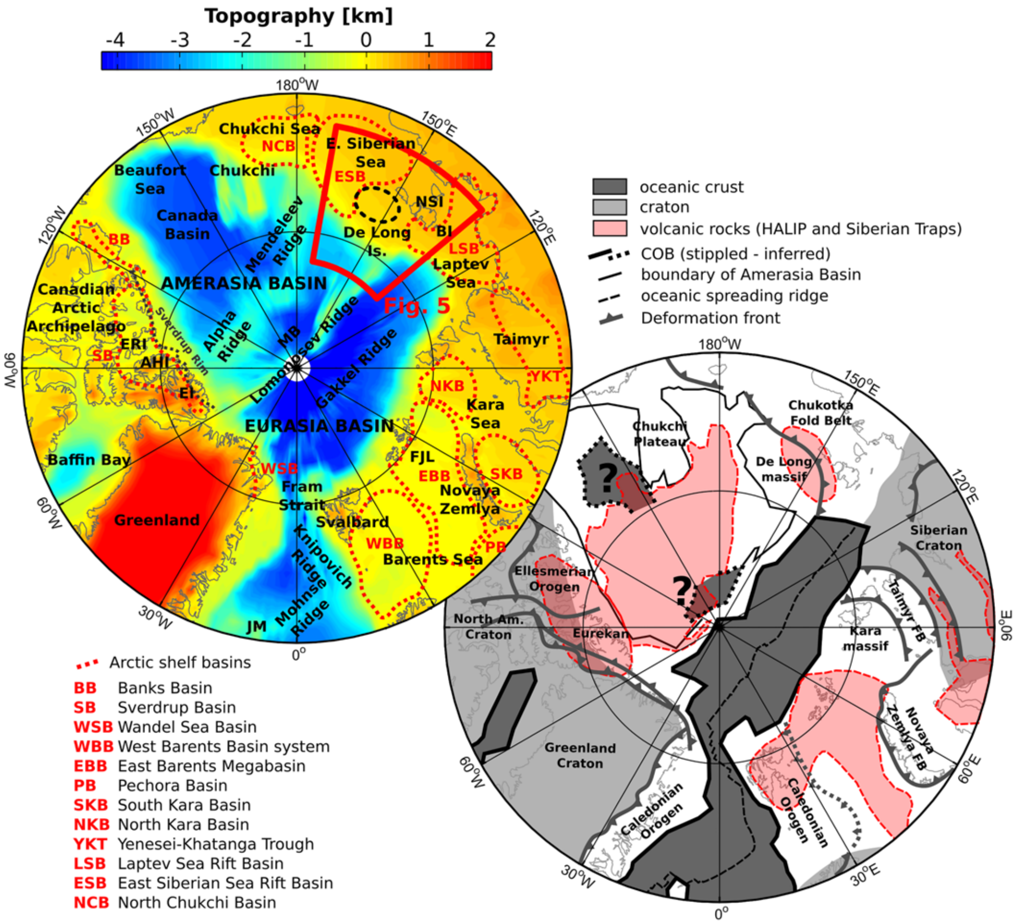

Fig. 1. Circum-Arctic overview maps. Left-hand panel: topography (ETOPO1) and geographical names. AHI, Axel Heiberg Island; BI, Bel'Kov Island; EI, Ellesmere Island; ERI, Ellef Ringnes Island; FJL, Franz Josef Land; JM, Jan Mayen; MB, Makarov Basin; NSI, New Siberian Islands. Outlined box shows location of overview map in Figure 5. Right-hand panel: main tectonic features (after Pease *et al.* 2014) showing oceanic crust, cratons, fold belts, magmatic provinces (Thórarinsson *et al.* 2015) and continent–ocean boundaries (COBs) (stippled where less constrained).

The land masses currently within the High Arctic were involved in the assemblage of the supercontinent Pangaea. There were several orogenic events in the region constituting the Arctic part of Pangaea (present day >60° N). The Mesoproterozoic–Neoproterozoic Grenville–Sveconorwegian orogenic event has been inferred to have affected parts of the Canadian Arctic, East Greenland, Svalbard, Franz Josef Land, Novaya Zemlya and Taimyr (Lorenz *et al.* 2012). During the Neoproterozoic–Cambrian Timanide Orogen, microcontinents and terranes were amalgamated along the northeastern Baltica margin (Gee & Pease 2004; Roberts & Olovyanishnikov 2004). The Timanide Orogen occurred prior to the Early Palaeozoic Caledonian Orogen, which involved the collision of the continents of Baltica and Laurentia in the area of East Greenland, western Scandinavia, the British Isles, NE America, northern Germany and NW Poland (Roberts 2003; Gee *et al.* 2008; Leslie *et al.* 2008). The contemporaneous Ellesmerian Orogen may be the Arctic continuation of the Caledonian Orogen along the northern Laurentia margin in the Devonian (Piepjohn & von Gosen this volume, in press; Gasser 2013; Gee 2015), during which multiple terranes (e.g. Chukotka, Chukchi and Arctic Alaska) may have accreted in a complex collisional system (Trettin 1987; Beranek *et al.* 2010; Lawver *et al.* 2011; Lemieux *et al.* 2011; Anfinson *et al.* 2012). Divergence between the recently accreted

Arctic terranes – now attached to Laurentia – and Siberia led to the collision between Siberia, NE Baltica and the Kazakhstan plate, which formed the Urals in the Late Carboniferous, and Taimyr (Otto & Bailey 1995; Cocks & Torsvik 2007; Pease & Scott 2009; Lawver *et al.* 2011; Zhang *et al.* 2013, 2015, this volume, in press *a*, *b*).

During the Permo-Triassic, Siberia and the Russian Arctic Shelf were dominated by magmatic activity associated with the Siberian Traps large igneous province, including the emplacement of extensive flood basalts and dyke swarms, and the formation of extensional rift basins (Reichow *et al.* 2002; Nikishin *et al.* 2010; Ivanov *et al.* 2013). The easternmost Russian Arctic terranes were assembled during the closure of the Mongol–Okhotsk Ocean in the Late Jurassic (Zorin 1999; Kravchinsky *et al.* 2002; Tomurtogoo *et al.* 2005). Novaya Zemlya is a fold belt formed in the Mesozoic (Curtis *et al.* this volume, in press; Zhang *et al.* this volume, in press *a*, *b*).

In the middle and upper Jurassic, the closure of the Cache Creek Ocean and, later, the subduction of the Farallon plate beneath western North America assembled further terranes and arcs to the Arctic Alaska terrane (Shephard *et al.* 2013). Extension along the Arctic Laurentian margin separated some of the assembled terranes from Laurentia, culminating in the opening of the Amerasia Basin in the Early Cretaceous (Grantz *et al.* 1998; Lawver *et al.* 2011). This was partly contemporaneous with the emplacement of the High Arctic Large Igneous Province (HALIP), during which large volumes of magmatic products were emplaced as flood basalts and dykes, now mainly located in the Amerasia Basin, but also in the Canadian Arctic Archipelago, Svalbard and Franz Josef Land (Maher 2001; Drachev & Saunders 2003; Buchan & Ernst 2006; Olesen *et al.* 2010; Grantz *et al.* 2011; Døssing *et al.* 2013*b*).

The Arctic Ocean is subdivided into the Amerasia Basin and the younger Eurasia Basin by the continental Lomonosov Ridge, which has crustal thicknesses (compare with Moho in Fig. 2, top right) of 25–30 km and extends from Greenland to the Siberian Shelf (Jokat *et al.* 1992; Grantz *et al.* 2001; Poselov *et al.* 2007). Whether the opening of the Amerasia Basin involved seafloor spreading, continental hyperextension, mantle exhumation or a combination of these processes is still debated. This is mainly a result of often unknown crustal affinity due to sparse or ambiguous geophysical and geological constraints, complicated by the thick sedimentary and igneous cover over up to 50% of the Amerasia Basin and by later crustal modification (Gaina *et al.* 2011, 2013; Saltus *et al.* 2011; Pease *et al.* 2014; Petrov *et al.* 2016). Samples from Alpha Ridge basalts are predominantly of Late Cretaceous age (82–88 Ma), while the Mendeleev Ridge has been dated at 127 Ma in the north and 260 Ma in the south, close to the Chukchi Borderland and the adjacent Canada Basin at 115–76 Ma (Van Wagoner *et al.* 1986; Jokat 2003; Brumley 2010; Morozov *et al.* 2013). Many models include oceanic crust in the most central part of the Canada Basin (Chian *et al.* 2016; Petrov *et al.* 2016); other workers also interpret the Makarov Basin as oceanic (Lebedeva-Ivanova *et al.* 2011; Døssing *et al.* 2013*b*; Pease *et al.* 2014) or even the entire Amerasia Basin as oceanic (Alvey *et al.* 2008; Gaina *et al.* 2013), although a large part of the Amerasia Basin is also regarded to be of transitional or hyperextended continental crust (Lebedeva-Ivanova *et al.* 2006; Grantz *et al.* 2011; Pease *et al.* 2014; Li *et al.* 2016; Petrov *et al.* 2016). Consequently, different opening scenarios have been proposed in the debate regarding the origin of the Amerasia Basin (Dutro 1981; Embry 1990; Lane 1997), including, but not limited to, an anticlockwise rotational opening during the rifting of Alaska from the Canadian Arctic margin along a large-scale strike-slip fault proximal to the present day Lomonosov Ridge (Embry 1991; Grantz *et al.* 2011) or a transform fault along the Alpha–Mendeleev Ridge (Doré *et al.* 2016).

From the Late Cretaceous to the Late Palaeogene, the Labrador Sea and Baffin Bay successively opened from south to north between Greenland and Canada (Chalmers & Pulvertaft 2001). This caused SW–NE movement and the counter-clockwise rotation of Greenland (Srivastava 1985; Okulitch & Trettin 1991; Trettin 1991*a*; Oakey & Chalmers 2012; Hosseinpour *et al.* 2013) and extension with associated alkaline magmatism in the Lincoln Sea, North Greenland and Ellesmere Island (Trettin & Parrish 1987; Estrada *et al.* 2010; Tegner *et al.* 2011; Thórarinsson *et al.* 2012, 2015). Seafloor spreading along the North Atlantic ridge caused Greenland to move northwards, terminated rifting and volcanism in Labrador Sea (Thórarinsson *et al.* 2011; Døssing *et al.* 2013*a*) and resulted in the Eurekan Orogen on Ellesmere Island and north Greenland in the Eocene (Tessensohn & Piepjohn 2000; Tegner *et al.* 2011; Oakey & Chalmers 2012; Piepjohn *et al.* 2016). Additional east–west compression caused by seafloor spreading along the Gakkel Ridge during the opening of the Eurasia Basin (Brozena *et al.* 2003; Glebovsky *et al.* 2006; Engen *et al.* 2008; Døssing *et al.* 2013*a*; Gaina *et al.* 2015) may have enhanced deformation in the Eurekan Orogen.

Lithospheric structure and pressure

As a result of this tectono-magmatic evolution, which included multiple compressional, extensional

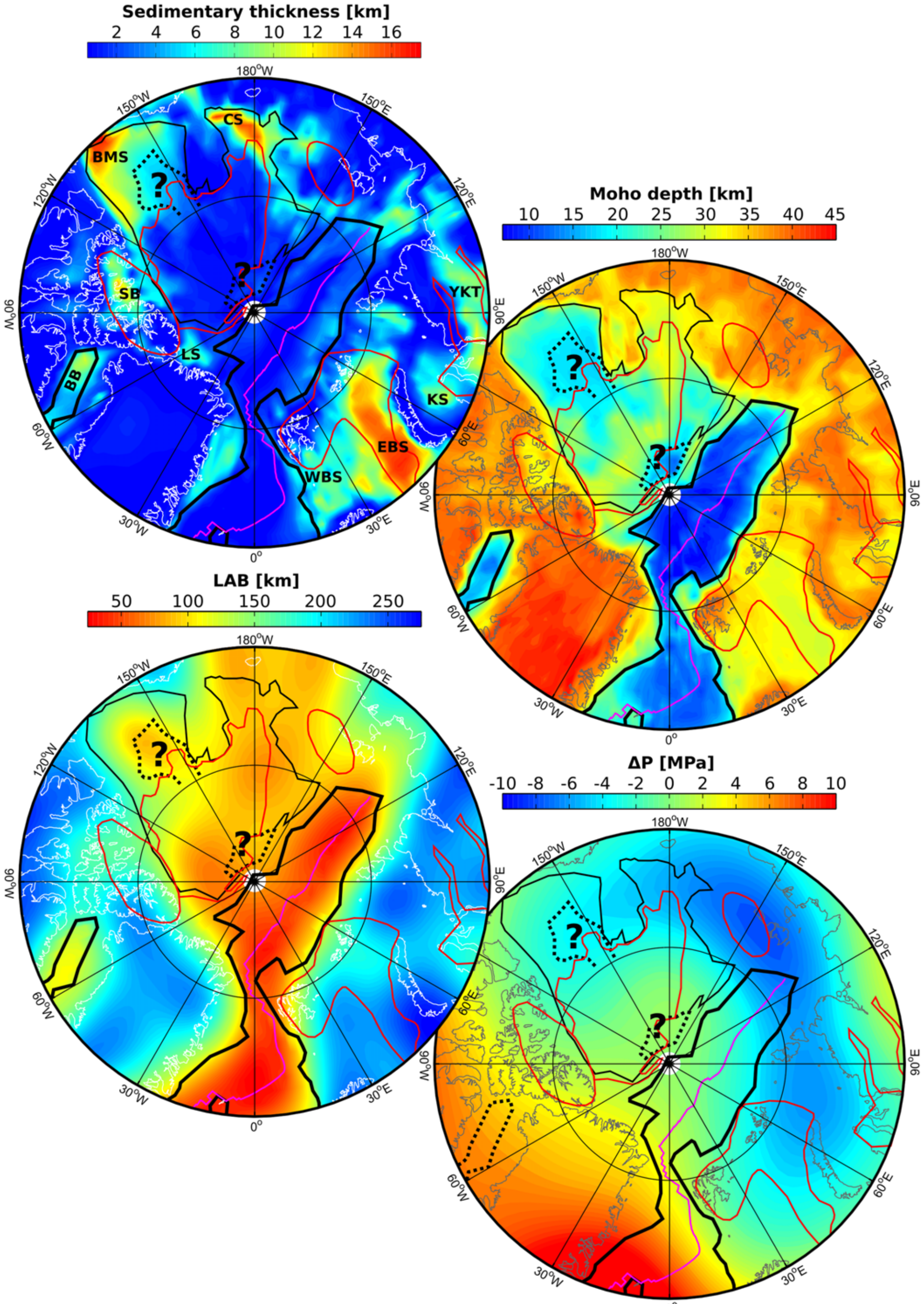

Fig. 2. Crustal and lithospheric structure in the High Arctic. Datasets from Lebedeva-Ivanova *et al.* (2016) and Schaeffer *et al.* (in review). Structural features from Pease *et al.* (2014) (see also Fig. 1). Thick black lines, continent–ocean boundaries; thin black line, boundary of the Amerasia Basin; red lines, volcanic rocks; magenta

and igneous events, the High Arctic consists of several distinct tectonic units, each of which is expressed in terms of their topography, sedimentary thickness, Moho and the thickness of the lithosphere (the depth to the LAB). The spatial variation in such structures results in lateral variations in the integrated mass of the vertical columns driving pressure differences – the source of geopotential stress. In this study, we combine recent geophysical datasets for the whole High Arctic region, including a newly compiled crustal model (Lebedeva-Ivanova *et al.* 2015, in review) and an LAB depth model (Schaeffer *et al.* submitted; Schaeffer & Lebedev 2015*b*). Together, these form the basis for our density model used to calculate the GPE and, ultimately, the corresponding geopotential stress field.

Crust and sedimentary basins

The crustal model of Lebedeva-Ivanova *et al.* (in review) describes the observed topography and bathymetry (Fig. 1, left), thicknesses and densities for a sedimentary and a crustal layer from 68 to 90° N (Fig. 2). Modifications were made at the boundaries to incorporate it into the global CRUST1.0 model (Laske *et al.* 2013). The Arctic model of Lebedeva-Ivanova *et al.* (in review) shows sedimentary basins (Fig. 2, top left) with depths ≥10 km in the southern Canada Basin/Beaufort–MacKenzie Sea (Stephenson *et al.* 1994*b*; Sippel *et al.* 2013), Chukchi Basin (Drachev 2011) and in the eastern Barents Sea (Drachev *et al.* 2010; Minakov *et al.* 2012; Klitzke *et al.* 2015). Other areas with locally substantial sedimentary thicknesses >5 km are observed in Baffin Bay (Funck *et al.* 2012; Suckro *et al.* 2012; Altenbernd *et al.* 2015), the Sverdrup Basin (Embry 1991; Embry & Beauchamp 2008; Oakey & Stephenson 2008; Schiffer *et al.* 2016), the Lincoln Sea (Jackson *et al.* 2010; Funck *et al.* 2011), the western Barents Sea (Ritzmann *et al.* 2007; Klitzke *et al.* 2015), the Kara Sea (Drachev *et al.* 2010) and the Russian Arctic Shelf (Drachev 2011; Drachev & Shkarubo this volume, in press).

The Amerasia Basin is one of the most debated features of the Arctic Ocean, with sections of possibly oceanic crust (e.g. the central Canada Basin and the Makarov Basin), others of hyperextended or intruded continental crust, and a large part covered by sediments and flood basalts of the Alpha–Mendeleev Ridge complex (Lebedeva-Ivanova *et al.* 2006, 2011; Jackson *et al.* 2010; Funck *et al.* 2011; Chian *et al.* 2016; Li *et al.* 2016). The Chukchi Borderland and the De Long Massif are continental terranes, separated and broken apart during the opening of the Amerasia Basin, with crustal thicknesses of up to 35 km subdividing other smaller basins. Although the crustal affinities of the Amerasia Basin are poorly constrained, the younger Eurasia Basin is clearly of oceanic origin and shows less complexity, at least from a kinematic point of view (Brozena *et al.* 2003; Engen *et al.* 2008). The continental shelf is generally much wider along the Russian (Moho at 35–40 km depth) and Barents Sea (Moho at 30–35 km depth) margins than along North America and Greenland.

The Arctic Ocean is surrounded by a number of orogenic belts. In the East Greenland Caledonides the Moho is estimated to be at a depth of up to 45–50 km (Artemieva & Thybo 2013; Schiffer *et al.* 2014, 2015*a*). Similar depths have been estimated for the Scandinavian Caledonides (Grad *et al.* 2009; Ebbing *et al.* 2012; Artemieva & Thybo 2013) and the Ellesmerian/Eurekan Orogen. A substantially shallower Moho has been estimated in the Sverdrup Basin at 30–35 km (Oakey & Stephenson 2008; Schiffer *et al.* 2016; Schiffer & Stephenson this volume, in press; Stephenson *et al.* this volume, in press). Beneath Svalbard, Novaya Zemlya and Taimyr, the Moho is estimated to be at up to 40 km depth or more (Ritzmann *et al.* 2007; Ivanova *et al.* 2011; Klitzke *et al.* 2015; Faleide *et al.* this volume, in review). The Moho beneath the stable cores of the surrounding continents is at depths of 35–45 km (Fig. 2).

Sub-lithospheric pressure

Lateral sub-lithospheric pressure variations that could be produced by mantle convection patterns or thermal or compositional anomalies in the sub-lithospheric mantle were permitted in the modelling. Such a pressure anomaly gives rise to dynamic topography. The Arctic crustal model from Lebedeva-Ivanova *et al.* (in review) provides an estimate of the dynamic topography. The model was translated into a sub-lithospheric pressure anomaly, which is required to produce the resulting dynamic uplift or subsidence. This pressure anomaly was smoothened to a harmonic degree of 36 (Fig. 2, bottom right) and integrated with a global sub-lithospheric pressure anomaly from Schiffer & Nielsen (2016), which may result in discrepancies at the edges of the study area at *c.* 70° N between the dataset used and the original datasets.

Fig 2. *(Continued)* line, oceanic spreading ridge. Upper left panel: sedimentary thickness; upper right panel: Moho depth; lower left panel: depth to lithosphere–asthenosphere boundary (LAB); lower right panel: sub-lithospheric pressure anomaly. BB, Baffin Bay; BMS, Beaufort–Mackenzie Sea; CS, Chukchi Sea; EBS, East Barents Sea; KS, Kara Sea; LS, Lincoln Sea; SB, Sverdrup Basin; WBS, West Barents Sea; YKT, Yenesei–Khatanga Trough.

The pressure anomaly and corresponding dynamic topography (Fig. 2, bottom right) is of long wavelength and shows a clear maximum of *c.* 10 MPa (corresponding to at most 400 m of uplift) in NE Greenland and Jan Mayen, approaching the Iceland melt anomaly. Slightly lower positive pressure anomalies of 0–5 MPa (0–150 m uplift) are present in Greenland and Arctic Canada, whereas a low amplitude negative anomaly of −6 to −2 MPa (*c.* 350–0 m subsidence) is located along the Russian Arctic Shelf. We note that the North Pole region demonstrates no anomalous mantle pressure.

Mantle lithosphere

The Earth's lithosphere plays a key part in the dynamic processes associated with plate tectonics because the base of the lithosphere is a first-order boundary separating the actively connecting, weak asthenosphere from the overlying rigid lithospheric plate. There are, however, a number of different ways to define the base of the strong lithospheric lid, including mechanical, compositional, rheological, thermal and anisotropic interpretations (Artemieva 2009; Eaton *et al.* 2009; Fischer *et al.* 2010). We use the LAB depth model (Fig. 2, bottom left) derived from a recent multi-mode (Lebedev & Van Der Hilst 2008; Schaeffer & Lebedev 2013, 2015*a*) surface waveform tomography model of the Arctic, AMISvArc, described in detail in Schaeffer *et al.* (2015*b*, in review). The authors utilized a common proxy for the LAB in studies based on surface waves, namely the depth at which the velocity anomalies dropped below the +2% fast velocity contour with respect to the one-dimensional mantle reference model AK135 (Kennett *et al.* 1995). This estimate is in many ways analogous to a thermal estimate for the LAB because the seismic velocities are dominantly sensitive to variations in temperature. This +2% fast criterion is optimum for identifying the depth to the LAB beneath stable continental regions; in regions with elevated temperatures, such as continental areas undergoing active deformation or beneath all but the oldest parts of oceanic plates, the +2% fast criterion is not satisfied because the observed velocities are less than the reference model (i.e. negative velocity anomalies).

The calculation for the geopotential stress field requires a continuous LAB depth model, so we combine the LAB model from Schaeffer *et al.* (in review) and Schaeffer & Lebedev (2015*b*) with other LAB constraints across the High Arctic. For example, in the eastern Russian Arctic, other models indicate an LAB depth of 50–100 km throughout the region (Conrad & Lithgow-Bertelloni 2006; Artemieva 2009) and therefore we assigned a constant thickness of 75 km across this region. In the oceanic domain, apart from the thicker lithosphere underlying the Canada Basin, we utilize an estimate based on plate age (Müller *et al.* 2008) for the lithospheric thickness using a standard half-space ocean age evolution model (Stein & Stein 1992) where applicable.

The original LAB model, computed on a triangular grid of tessellated knots (Wang & Dahlen 1995) with an average spacing of *c.* 280 km, was expanded onto spherical harmonics up to a degree of 64. The LAB depth model (Fig. 2, bottom left) roughly follows the standard ocean age dependent depth model with <50 km at mid-ocean ridges and increasing to *c.* 120 km at the continent–ocean boundaries. In Baffin Bay, the LAB is at *c.* 120 km depth, corresponding to old oceanic lithosphere at the extinct spreading ridge. The Amerasia Basin also has relatively thin lithosphere at *c.* 75 km depth north of Ellesmere Island and North Greenland, in the Canada Basin and along the Mendeleev Ridge, *c.* 100 km elsewhere along the Alpha–Mendeleev Ridge and up to *c.* 150 km at the margins of the Canada Basin. The continent–ocean boundaries (Fig. 2, thick black lines; stippled where alleged or extinct; Müller *et al.* 2008) are clearly defined by steep LAB depth gradients from thinner oceanic to thicker continental lithosphere in most places. Exceptions are observed along the eastern Russian shelf, including the Chukchi Plateau and the De Long Massif, where thin lithosphere continues far inside the continental interior. This steep gradient is also lacking in the Canada Basin, where the lithosphere is up to 200 km thick at the edges of the basin – thicker than typical oceanic lithosphere – and gradually thins to a minimum of *c.* 90 km in the centre.

The northwesternmost part of Svalbard and the possible continental extension to the north show extremely thin lithosphere, atypical of continents, also observed by previous workers (Klitzke *et al.* 2015). The concluding observation is that the presumed boundaries (Müller *et al.* 2008) between the continents and the Amerasia Basin (Fig. 2, thin black lines are an interpretation of the continent–ocean boundaries from Pease *et al.* 2014) do not always clearly coincide with a change in LAB depth. Thin lithosphere is sometimes observed outside the proposed continent–ocean boundaries and thicker lithosphere is often observed within the basin. This shows that the position of the continent–ocean boundaries is either not well known, or the definition fails in some regions of the Arctic. Greenland, southern Ellesmere Island, Arctic Canada (south of the Sverdrup Basin), the Barents Sea, Novaya Zemlya, Kara Sea, Taimyr and western Siberia have very thick lithosphere with an LAB at >225 km depth, but with significant internal variation.

Geopotential stress field

Our methods follow those of Schiffer & Nielsen (2016) and Nielsen *et al.* (2014) and the most important elements are summarized here. The GPE is the integral over the vertical column of a lithostatic pressure anomaly, defined as:

$$GPE = \int_{-H}^{L} (L - z)\Delta\rho g \, dz,$$

where L is the depth up to which density variations are incorporated, H is the topographic elevation, $\Delta\rho$ is the vertical density anomaly with respect to a reference lithosphere, g is the gravitational acceleration, z is depth. L, H and z are in "m", g in "$\mathrm{m} \times \mathrm{s}^{-2}$" and ρ in "$\mathrm{kg} \times \mathrm{m}^{-3}$" and GPE in "$\mathrm{N} \times \mathrm{m}^{-1}$".

The density column of the mantle lithosphere was defined by the thermal expansion of peridotite along a conductive geotherm using a reference thermal expansion coefficient of $\alpha = 2.4 \times 10^{-5}$ K^{-1} and a reference density of $3350\,\mathrm{kg\,m}^{-3}$. The geotherm was defined by a surface temperature of 0°C, a temperature at the LAB by the adiabatic mantle geotherm of $[\partial T/\partial z] = 0.6°\mathrm{C\,km}^{-1}$ (McKenzie & Bickle 1988), a reference potential temperature of 1315°C (McKenzie *et al.* 2005) and representative thermal conductivities and heat production rates for sediments, crust and lithosphere (Schiffer & Nielsen 2016). The expansion coefficient and thermal conductivity are regarded as temperature dependent (Bouhifd *et al.* 1996; McKenzie *et al.* 2005). Horizontal gradients of GPE are a source of deviatoric stress in the lithosphere. To calculate these stresses, a thin sheet approximation of the lithosphere (Bird & Piper 1980; England & McKenzie 1982; England & Houseman 1986) was assumed. Horizontal tractions at the base of the lithosphere were neglected because mantle flow patterns and mechanical coupling between the asthenosphere and lithosphere are poorly constrained and generally much less important than vertical stress.

Given this, the equations of equilibrium of stresses are:

$$\begin{pmatrix} \dfrac{\partial\bar{\tau}_{xx}}{\partial x} + \dfrac{\partial\bar{\tau}_{xy}}{\partial y} = -\dfrac{1}{L}\left(\dfrac{\partial GPE}{\partial x} + L\dfrac{\partial\bar{\tau}_{zz}}{\partial x}\right) \\ \dfrac{\partial\bar{\tau}_{yx}}{\partial x} + \dfrac{\partial\bar{\tau}_{yy}}{\partial y} = -\dfrac{1}{L}\left(\dfrac{\partial GPE}{\partial y} + L\dfrac{\partial\bar{\tau}_{zz}}{\partial y}\right) \end{pmatrix} \quad (2)$$

Here, x and y are the local horizontal coordinates, $\bar{\tau}$ represents the depth-integrated deviatoric stresses, $\bar{\tau}_{xx}, \bar{\tau}_{yy}, \bar{\tau}_{xy}, \bar{\tau}_{yx}$ are the horizontal deviatoric stresses, L is the reference depth and $\bar{\tau}_{zz}$ is a sub-lithospheric pressure anomaly acting vertically at the base of the lithosphere (radial tractions), which was derived from the dynamic topography grid.

The final equations of equilibrium of stresses (equation 2) were solved using the finite element method in the following way (Zienkiewicz 1977). The spherical Earth is represented by a dense grid of flat, thick, triangles with an elastic rheology. The material parameters of each element consist of Young's modulus (E), Poisson's ratio (ν) and a uniform thickness (L). Interested readers are referred to Schiffer & Nielsen (2016) for further information.

The elastic shell approximates the strength-carrying layer of the Earth's lithosphere, which supports stresses. Lateral thickness variations of this layer cause stress refraction, which influences the stress directions, but because of the smooth thickness variations in the present model such refraction effects are small. The primary influence of variations in the thickness of the strength-carrying layer is the magnitude of the stress flux, which does not influence the orientation of the stress field.

We follow common approaches to calculate the GPE and the corresponding stress field and use a reference depth of $L = 100$ km, corresponding to the upper lithospheric structure as the main stress-carrying layer (Flesch *et al.* 2001; Ghosh *et al.* 2008). In addition, a reference depth of 50 km – corresponding to mostly crustal structure – is used to investigate the differences between shallow and deep sources of geopotential stress (Fig. 3).

We use a spatially averaged representation of the WSM. A location is attributed a stress orientation if at least three high-quality measurements (quality A, B and C of the WSM) are within a radius of up to 250 km, although smaller distances above 50 km are preferred. Again, details are described in Schiffer & Nielsen (2016). The resulting GPE, stress field and a comparison with the WSM are shown in Figure 4 (upper panels).

Dykes and extensional structures in the High Arctic

Palaeostress indicators can be found across the High Arctic (Fig. 4, lower panels). Dykes are usually emplaced parallel to the maximum horizontal compressive stress. Large systems of extensional basins may also be oriented along the most compressive horizontal stress direction, although these may be influenced by existing and inherited rift structures. In Figure 4 (lower panels), we show the Phanerozoic dykes and rift systems in the High Arctic of known age. Figure 1 shows the location of these basins.

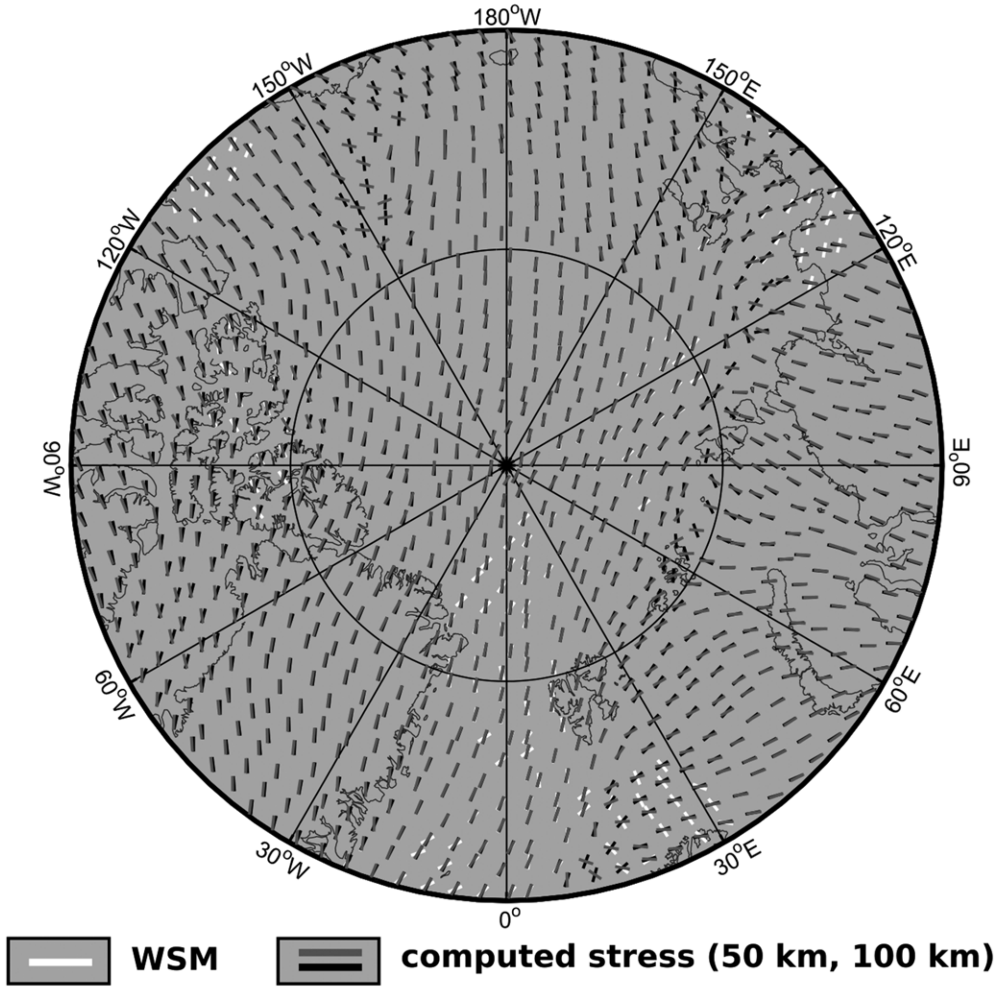

Fig. 3. Comparison of the geopotential stress field using the geopotential energy to a depth of 50 km (light grey) – representing mostly crustal structures – and to a depth of 100 km (black) – representing lithospheric structures – with a smoothed version of the World Stress Map (WSM, white). The shallow stress field (grey) and deep stress field (black) coincide very well in oceanic and intraplate areas, but deviate along the passive margins, such as the Chukchi margin to the Canada Basin, the Canadian polar margin, the East Siberian Sea and Laptev Sea, as well as the Barents Sea–North Atlantic margin and around Franz Josef Land. If differences are observed, the shallow stress field usually fits the WSM better than the deep stress field, especially in the western Barents Sea and the Canadian Arctic Archipelago.

Ordovician to Carboniferous

The oldest of the Phanerozoic rift basins in the Arctic include the Pechora Basin (Klimenko *et al.* 2011) and the North Kara Basin (Stoupakova *et al.* 2011), which both started extending in the Ordovician (Nikishin *et al.* 1996; Gee & Pease 2004; Drachev 2016). The Pechora Basin experienced a second phase of extension in the Devonian. The North Kara Basin has a predominant west–east fault orientation, whereas the Pechora Basin has a NNW–SSE orientation. Rifting in the East Barents megabasin started in the late Devonian with a SW–NE-oriented rift axis in the southwestern part and west–east orientation in the northeastern part (Nikishin *et al.* 1996; Drachev *et al.* 2010; Drachev 2016). Normal fault systems in the western Barents Sea formed in the Carboniferous and are generally NW–SE-trending (Gudlaugsson *et al.* 1998; Faleide *et al.* 2008; Henriksen *et al.* 2011). The Sverdrup

Basin formed initially as a result of lithospheric relaxation of the Ellesmerian Orogen, then as an active rift in the Carboniferous to Permian (Embry 1991) and, finally, as a consequence of thermal subsidence (Stephenson *et al.* 1994*a*). The Wandel Sea Basin in NE Greenland opened at a similar time during the Carboniferous and Permian and is related to rifting between Greenland and Scandinavia (Håkansson & Stemmerik 1989; Stemmerik *et al.* 1998).

Permo-Triassic

Siberian Trap magmatism is one of the largest magmatic events on Earth, stretching from around 60–120° E and 50–75° N and dated at *c.* 251 Ma (Reichow *et al.* 2002, 2009; Burgess & Bowring 2014). Large-scale north–south-trending extensional fault systems in the West Siberian Basin developed contemporaneously, indicating the regional-scale orientation of the stress field during this time (Reichow *et al.* 2002). NNW–SSE-trending dykes and associated normal faults on Bel'-Kov Island (the westernmost New Siberian Island, Fig. 1) also date to *c.* 251 Ma and have been linked with the Siberian Trap magmatic event (Kuzmichev & Pease 2007; Danukalova *et al.* 2014). Dyke swarms on Taimyr have been dated to slightly older (280 Ma; Pease & Vernikovsky 2000) and slightly younger (220–250 Ma; Walderhaug *et al.* 2005). Reichow *et al.* (2016) revised this work and presented ages of intrusions on the Taimyr Peninsula coinciding with the Siberian Traps. Their NE–SW and ENE–WSW orientations are very different from the north–south extensional rift systems in the area of the Siberian Traps. To the north of the East Siberian Basin, the Yenisei–Khatanga Trough opened along a very similar axis to the Taimyr dyke swarm (Drachev *et al.* 2010).

Early Cretaceous

In the Early Cretaceous, voluminous magmatism occurred in many parts of the High Arctic, forming the HALIP. Part of this is a large dyke swarm emplaced into the Amerasia Basin, the Canadian and Greenland Arctic shelves and borderlands, Svalbard and Franz Josef Land (Drachev & Saunders 2003; Buchan & Ernst 2006). Dykes, sills and lavas are abundant in the Canadian Arctic Archipelago and cover a long time span, but with a main phase of basaltic volcanism at *c.* 127–115 Ma. On Ellef Ringnes Island, a major dyke and sill swarm is dated at 127–121 Ma and mainly strikes NE–SW (Evenchick *et al.* 2015). On Axel Heiberg Island the Early Cretaceous dyke swarm mainly strikes north–south (Buchan & Ernst 2006), has been dated at 123 Ma (Pease & Nobre Silva 2015) and can be directly linked to magnetic signatures that extend into the offshore domain (Anudu *et al.* 2016). On Ellesmere Island, HALIP volcanism and dykes range from *c.* 122 to 74 Ma (Estrada & Henjes-Kunst 2013). Dykes and sills also outcrop on Svalbard (Senger *et al.* 2014) and can be extended offshore (Olesen *et al.* 2010) and into the Barents Sea (Polteau *et al.* 2016). Similarly, a major dyke swarm has been mapped on Franz Josef Land (Dibner 1998), with peak ages at 138–110 Ma, and can also be extended offshore using aeromagnetic data (Glebovsky *et al.* 2006; Minakov *et al.* 2012; Døssing *et al.* 2013*b*). The dykes in the European part of the Arctic have been dated at 130–110 Ma (Corfu *et al.* 2013).

Døssing *et al.* (2013*b*) used aeromagnetic data to interpret a large offshore dyke swarm between (and partly within) Alpha Ridge, Lomonosov Ridge, Ellesmere Island and Makarov Basin; its age is unconstrained, but given the clear spatial relation of this dyke swarm with the Franz Josef Land dykes in palaeogeographical reconstructions, an Early Cretaceous age is very likely. Predominant orientations of other dyke swarms are NNE–SSW in the western Sverdrup Basin and the Alpha Ridge, north–south to NW–SE along the northern coastline of Ellesmere Island and Axel Heiberg Island, NW–SE on Franz Josef Land and NNW–SSE in the Barents Sea, and roughly north–south on and around Svalbard. These are interpreted to form a radiating dyke swarm in some plate tectonic reconstructions (Buchan & Ernst 2006; Døssing *et al.* 2013*b*).

The Amerasia Basin opened during the Early Cretaceous (although this is debated) and the rift axes are oriented north–south to NNW–SSE (Nikishin *et al.* 2014; Petrov *et al.* 2016). The Canada Basin is interpreted by some researchers to be partly formed by oceanic spreading (e.g. Chian *et al.* 2016; Pease *et al.* 2014; Petrov *et al.* 2016). Banks Basin and the Sverdrup Rim (see Fig. 1), both oriented parallel to the shelf edge, developed as a consequence of rifting and the subsequent opening of the Amerasia Basin (Embry & Dixon 1990).

Figure 5 presents further evidence for the orientation of dykes and a graben structure on Bennett Island, part of the De Long Islands at *c.* 150° E on the Russian Arctic Shelf (Vol'nov & Sorokov 1961). Bennett Island is composed of lower Palaeozoic sediments overlain by flood basalts that have been dated at 119–112 Ma and interpreted as part of the HALIP (Drachev & Saunders 2003; Tegner & Pease 2014). Two dykes at the western end of the island (Cape Emma) strike *c.* NE–SW and are interpreted as coeval with the flood basalt event (Fig. 5a, b). The southeastern end of the island displays a graben structure (Fig. 5c) in a similar

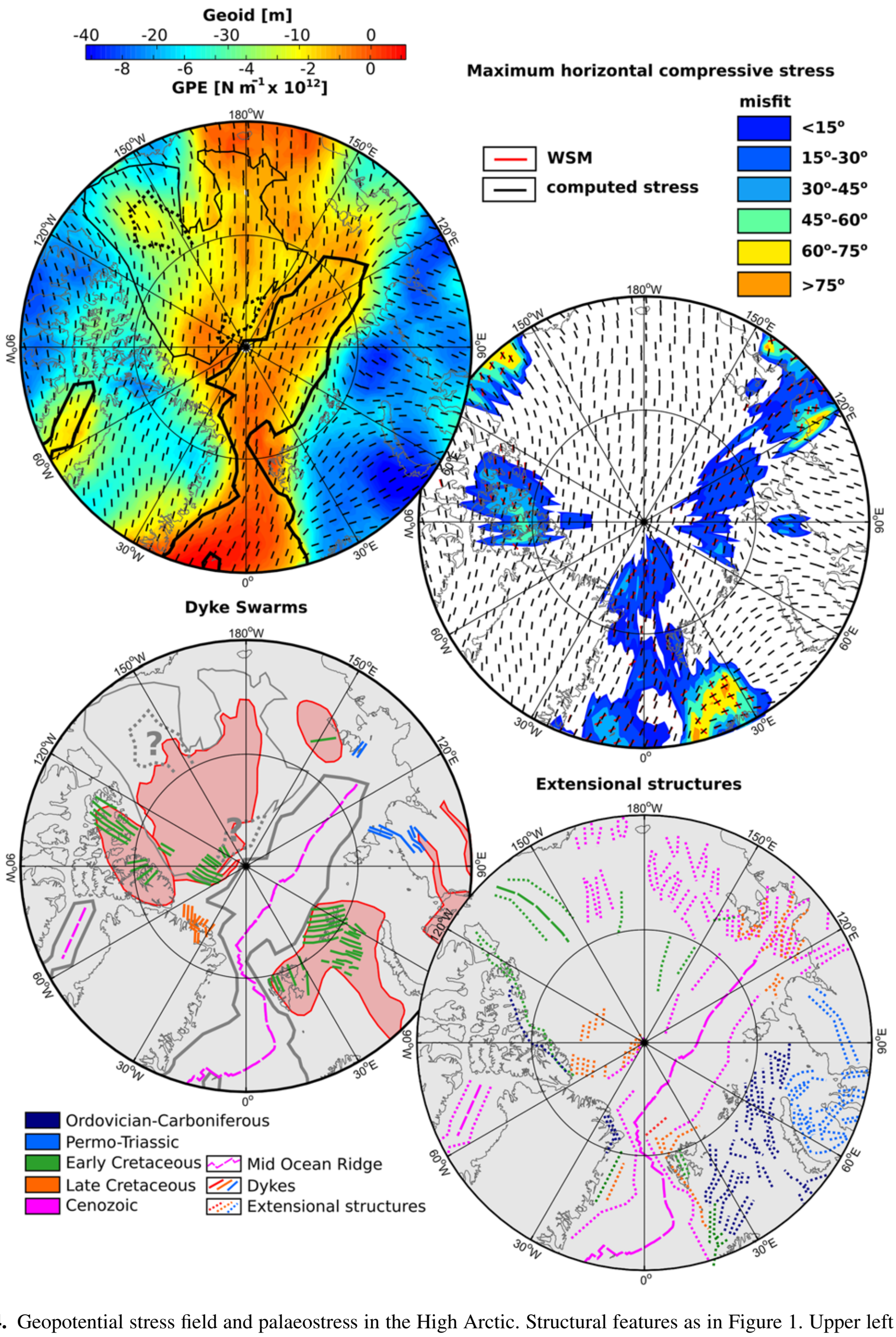

Fig. 4. Geopotential stress field and palaeostress in the High Arctic. Structural features as in Figure 1. Upper left panel: geopotential energy model, corresponding geoid anomaly and computed compressive deviatoric stress directions (black lines). Upper right panel: computed compressive deviatoric stress directions (black lines) and underlying average stress directions of the World Stress Map (WSM; red lines). A contour map of the angular misfit is shown in the background. White areas indicate where the WSM has insufficient or no data. Only every fourth stress grid point is shown as black and red lines for clarity. Lower left panel: High Arctic dykes (coloured lines) and magmatic provinces (red shading). HALIP dykes in the Canadian Arctic, Greenland, Svalbard and Franz Josef Land (green) are from Buchan & Ernst (2006), Olesen *et al.* (2010), Døssing *et al.* (2013*b*) and Polteau *et al.* (2016). The

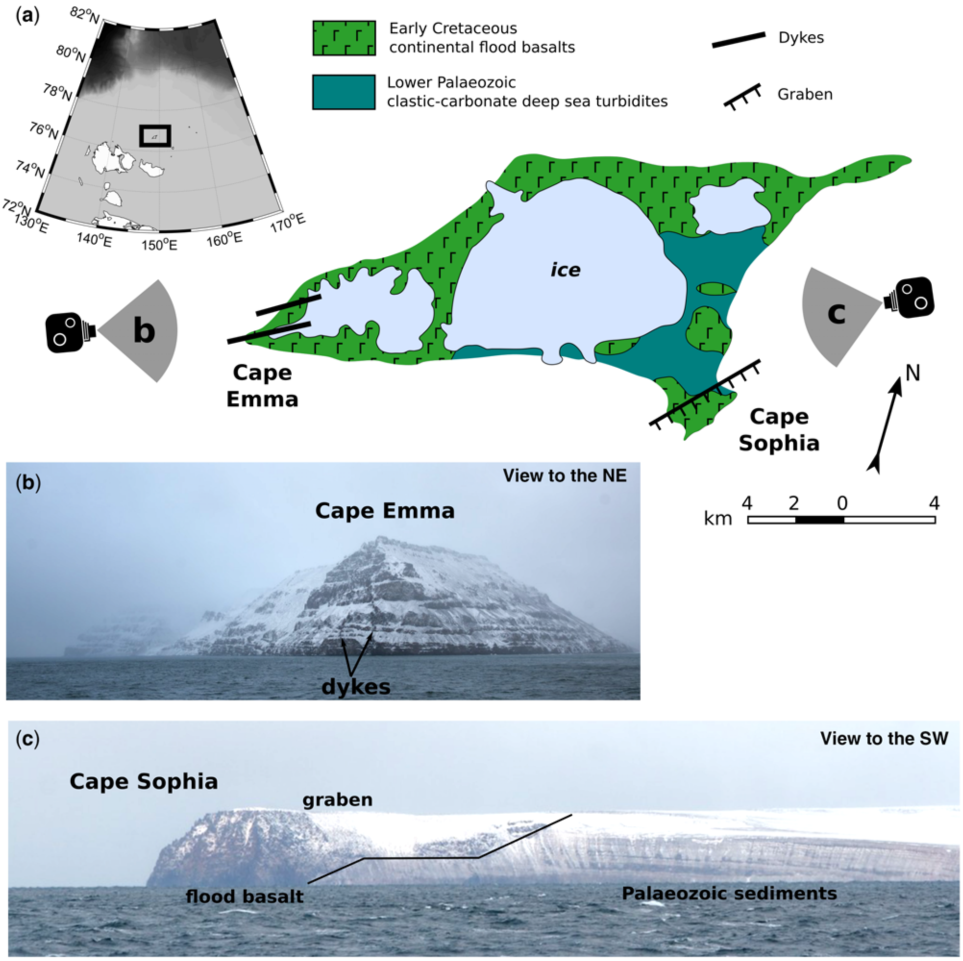

Fig. 5. Bennett Island. (**a**) Geological map of Bennett Island. Inset, overview map. Camera positions for parts (b) and (c) are indicated. (**b**) Photo of Cape Emma with view to the NE showing two dykes. (**c**) Photo of Cape Sophia with view to the SW showing a graben structure (indicated by black line) filled with flood basalts (see geological map in part (a)).

orientation that accommodated the basaltic eruptions. We interpret these structures on Bennett Island as indicative of NW–SE extension in the Early Cretaceous.

Late Cretaceous

Three suites of Late Cretaceous alkaline dykes are located on the north Greenland margin. One

Fig. 4. (*Continued*) dykes and rift axis on Bennett Island are from this study. The Late Cretaceous dyke swarms in north Greenland (orange) are from (Thórarinsson *et al.* 2015). The Permo-Triassic on the Taimyr peninsula (blue) are from Pease & Vernikovsky (2000) and Walderhaug *et al.* (2005). The Permo-Triassic dykes in the Russian Arctic Islands (blue) are from Kuzmichev & Pease (2007) and Danukalova *et al.* (2014). Lower right panel: extensional structures (coloured dotted lines) as palaeostress markers. Late Cretaceous extensional structures in the Alpha Mendeleev Ridge/Eastern Amerasia Basin from Døssing *et al.* (2013*a*). Rift systems in NE Greenland and the western Barents Sea from Faleide *et al.* (2008) and Klitzke *et al.* (2015). Rift systems in the eastern Barents Sea from Marello *et al.* (2013). 'Siberian Traps' rift systems after Reichow *et al.* (2009). Cenozoic rift systems of the eastern Arctic Russian shelf from Drachev (2011). Palaeomargins and spreading centre of the Canada Basin from Grantz *et al.* (2011). Sverdrup Basin axis and Sverdrup Rim from Embry (1991). Wandel Sea Basin structures from Stemmerik *et al.* (1998). Banks Basin outline from Trettin (1991*b*). Amerasia Basin rift axes from Nikishin *et al.* (2014).

population is east–west oriented, another north–south and the third NW–SE, and all have similar ages (85–81 Ma) (Buchan & Ernst 2006; Thórarinsson *et al.* 2015). The north–south orientation of one dyke population appears to be parallel to the rift axis of the Eurasia Basin, whereas the NW–SE orientation of the other population may relate to mapped extensional structures along the Alpha and Lomonosov ridges (Døssing *et al.* 2013*a*; Thórarinsson *et al.* 2015).

Pervasive, roughly north–south-striking extensional fault systems are distributed over large parts of the Russian Arctic Shelf from *c.* 150° W to 120° E. The Laptev Sea Basin defines the westernmost set of normal faults within the Laptev rift system; its easternmost part is represented by the New Siberian Basin located north of the New Siberian Islands. The Laptev Sea Basin reflects continental rifting along the landward extension of the present day Gakkel Ridge during the Late Cretaceous and Early Eocene (Engen *et al.* 2003; Drachev 2011; Drachev & Shkarubo this volume, in press). Continental break-up occurred along the Gakkel Ridge at *c.* 56 Ma, but might have failed to propagate into the Laptev Sea (Franke *et al.* 2001; Drachev *et al.* 2003; Van Wijk & Blackman 2005; Franke & Hinz 2009) and the spreading ridge was probably aborted in the mid-Cenozoic. It was rejuvenated during the middle Miocene through middle Pleistocene (Drachev 2011).

Cenozoic

During the Eocene, seafloor spreading started in the NE Atlantic and in the Eurasia Basin. The present day passive margins away from transform margins may represent the general direction of the stress field at the time of break-up. Therefore we use the passive margins as weak indicators of palaeostress orientations, even though it is possible that inheritance plays an important part in the development of rifts. In the present day NE Atlantic, Pangaea broke apart at *c.* 53 Ma, while at *c.* 25 Ma a NE Atlantic ridge jump caused the separation of Jan Mayen (Mosar *et al.* 2002; Nielsen *et al.* 2007; Tegner *et al.* 2008; Gernigon *et al.* 2015). The Eurasia Basin opened simultaneously as an elongated ocean basin along the future ultra-slow-spreading Gakkel Ridge (Brozena *et al.* 2003; Gaina *et al.* 2015). The Fram Strait region developed from the De Geer transform fault, connecting the Arctic and the North Atlantic from the Early Eocene (Engen *et al.* 2008; Doré *et al.* 2016). It displays a complex system of transform faults, fracture zones and oblique spreading ridges oriented nearly perpendicular to the North Atlantic and Gakkel ridges; seafloor spreading has been active since the Miocene (Engen *et al.* 2008; Doré *et al.* 2016). This complexity compromises a detailed interpretation of the palaeostress field. The East Siberian Sea is much less studied than the Laptev Sea, but overall is considered to have experienced much less extension. It subsided post-Late Cretaceous and, during the initial phases of seafloor spreading along the Gakkel Ridge from the Eocene, the East Siberian Basin is suggested to have formed through large-scale extensional/transtensional deformation, which terminated in the Middle–Late Miocene (Franke *et al.* 2004; Franke & Hinz 2009; Drachev 2011, 2016; Drachev & Shkarubo this volume, in press).

Results

Geopotential stress field

We calculated the GPE (Fig. 4, upper left) as one source of lithospheric stress in the High Arctic. The GPE distribution identifies distinct provinces. The cratons exhibit very low GPE values, which is the result of deep lithospheric keels, low topography and the presence of sedimentary basins. Conversely, a high GPE is caused by high topography (e.g. East Greenland, Ellesmere Island, as well as the Lomonosov, Alpha, Gakkel and Mid-Atlantic ridges), a thin mantle lithosphere (ocean basins, parts of the Amerasia Basin, Bering Strait region at *c.* 180° E/W) and a lack of sedimentary cover.

The geopotential stress field is used as an approximation of the present day lithospheric stress field (Fig. 4, upper panel). The stresses are aligned with the active Gakkel Ridge and the Mid-Atlantic Ridge. This also applies to the extinct spreading ridge in northern Baffin Bay. However, north of Jan Mayen, along the Mohns and Knipovich ridges where seafloor spreading occurs along a highly complex and oblique spreading ridge with a strong translational component, the calculated and observed stress orientation deviates from the ridge axis. The stress field appears to be uniform throughout the oceanic Eurasia Basin. The same is observed in the Amerasia Basin, where the equally uniform stress field is slightly rotated anticlockwise by 10–20° relative to the Eurasia Basin. The Lomonosov Ridge appears to demarcate the boundary between these two stress regimes.

The stress orientation changes from north–south along the East Greenland coastline to a more NW–NE direction in the interior of the continent and to north–south in North Greenland and Ellesmere Island. In the eastern part of the Canadian Arctic Archipelago, the principle compressive stresses are coast-parallel, before changing to a north–south orientation at about 130° W. This trend is observed along the entire shelf to *c.* 130° E, with slight complexity at 150° E. At 130° E the stress field changes to a NE–SW orientation, pointing towards the GPE low and corresponding to thick cratonic lithosphere. Along the western Russian Arctic Shelf the stress field changes gradually anticlockwise from the initial NE–SW direction at Taimyr to a west–east orientation across almost the entire western Barents Sea.

Comparison with the World Stress Map

The WSM is a global compilation of stress field observations, including several *in situ* measurements and the analysis of focal mechanisms from earthquakes (Heidbach *et al.* 2010). Owing to the remote location of the study region, stress measurements are mostly based on the calculation of focal mechanisms where available, especially in offshore areas such as along the Gakkel Ridge, North Atlantic Ridge and in Baffin Bay, but also in East Siberia. We note that single focal mechanisms do contribute to the WSM elsewhere. Borehole breakouts are most abundant in the western Barents Sea and in the Alaska and Canadian polar margins. A small subset of drill-induced fracturing data are also included in the western Barents Sea. Comparison with the WSM shows that the computed stresses in most regions are in fairly close agreement, with some exceptions (Fig. 4, upper right).

Misfits can have several causes: (1) the assumed lithospheric density structure for the area may be incorrect and model errors or coarse resolution can produce inaccuracies within the GPE model; (2) the sub-lithospheric pressure anomaly and resulting dynamic topography may have errors that propagate to the GPE model; and (3) intraplate seismicity in the High Arctic is sparse and weak, thus high-quality observations of the stress directions may be limited (*cf.* the WSM) and can result in poor observational quality. We also acknowledge differences due to the different methods used to estimate the stress field orientation. Different methods may be sensitive to different depth ranges – for example, focal mechanisms are more representative of crustal- to lithospheric-scale stress, whereas borehole breakouts may only account for shallower depths of a few kilometre. In addition, there might be far-field tectonic forces acting on the lithospheric stress field today, e.g. from distant subduction and collision zones.

We identify three regions of substantial misfit between the observed stresses (WSM) and the computed geopotential stress field (Fig. 3; Fig. 4, upper right). In the western Barents Sea (between Svalbard and Norway), the stress field undergoes a radical change from a direction parallel to the North Atlantic passive margin to a direction almost perpendicular to this further inside the Barents Sea. This deviation in the stress field is possibly related to the observed rapid change in LAB depth from >200 km in the east to *c.* 100 km in the oceanic domain in the west. The WSM, however, shows a corresponding change in stress orientation much further within the continental interior.

The East Siberian margin at *c.* 120–130° E shows a similar misfit at the edge of a rather steep LAB depth gradient (225 km in the interior of the continent to <150 km to the north and east). A different LAB depth architecture in this region, or any of the above-mentioned possible errors, might explain this misfit.

Another area of substantial misfit is observed in the Beaufort Sea, between the western Canadian Arctic Islands and the Brooks Range at *c.* 130–140° W. The WSM shows east–west-oriented stress, whereas the computed stress field indicates a continuous north–south orientation. A steeper east–west LAB depth gradient could produce such a stress field.

An interesting observation is that two of these regions are spatially co-located with regions where borehole breakout data are the dominant contribution to the WSM (the western Barents Sea and the Beaufort Sea). This may suggest that in these regions the WSM is dominantly sensitive to shallower structures where stress orientations are different from those in the deeper crust and lithosphere.

As indicated, the areas of high misfit are typically localized at steep edges of thick lithosphere. In a previous study, an LAB model was iteratively adjusted to fit the observed stress field (cf. Schiffer & Nielsen 2016). The final model showed much smoother LAB depth gradients and a correspondingly better fit with the WSM. Exploring what effect the absolute LAB depth and LAB gradient have on the GPE are beyond the scope of this paper, but will be examined in detail in subsequent work. For some regions, a lack of data limits the WSM; this is especially true for the predominant use of focal mechanisms and the lack of independent stress field measurements.

Excluding the regions of large misfit, the computed and observed stress directions match very closely and are sufficient to argue that the geopotential stress field is a robust representation. It is important to note that the modelling of the geopotential stress field presented in this study covers the entire High Arctic region, whereas the WSM is limited to areas of active seismicity (i.e. seafloor spreading ridges) and some limited areas of intraplate seismicity and boreholes.

Figure 3 shows a comparison between the calculated shallow (50 km) and deep (100 km) geopotential stress field, together with the smoothed WSM. As previously observed, the geopotential stress field for both depths as well as the WSM closely match in most regions. The deviation between both stress fields is observed dominantly along passive margins, such as the margin of Chukchi to the Canada Basin, in the Laptev Sea and East Siberian Sea, along the Canadian polar margin and the Barents Sea Atlantic margin, and the Amerasia Basin margin close to Franz Josef Land. Across the entire High Arctic, the shallow geopotential stress field fits better (24.27° azimuthal misfit) than the deep geopotential stress field (27.66° misfit); this probably reflects the generally shallower sensitivity of the WSM. In the following discussion, we choose to represent the present day lithospheric stress field with the geopotential stress field utilizing density structure to a depth of 100 km, which we interpret to be more representative of the lithosphere-scale tectonic structure.

Comparison with dyke swarms and rifts

The geopotential stress field (Fig. 4) can be compared with dyke swarms and extensional basins that act as palaeostress markers. Figure 6 shows the Phanerozoic extensional rift systems and dyke swarms of different ages in the High Arctic described here and separately shown in Figure 4 (lowermost panel) compared with the computed geopotential stress field (black lines). This allows for a direct comparison and evaluation of regions of better or worse fit.

The oldest observed rift systems in the western and eastern Barents Sea (Fig. 6, dark blue) show poor agreement with the present day stress field and hence we suggest that the Ordovician to Carboniferous stress field associated with these rift systems has been subsequently modified. The axis of the Sverdrup Basin is almost perpendicular to the computed geopotential stress field. Indeed, both regions have experienced a complex tectonic evolution, with multiple reconfigurations of the stress regime, including multiple extensional and orogenic events such as the Cenozoic Eurekan Orogeny (Piepjohn *et al.* 2016).

Permo-Triassic geological structures show generally good alignment with the contemporary geopotential stress directions in the Siberian Trap region and Taimyr (Fig. 6, light blue). It appears that the stress field has not changed significantly in these regions of good fit, even though Late Triassic folding has been reported from the Taimyr Peninsula (Inger *et al.* 1999; Torsvik & Andersen 2002).

None of the Early Cretaceous dyke swarms associated with the HALIP shows a clear alignment with the geopotential stress field today (Fig. 6, green). By contrast, those in the Amerasia Basin (Nikishin *et al.* 2014) and Banks Basin (Trettin 1991*b*) in the Canadian Arctic show relatively good agreement. This indicates that rifting and dyking occurred under different stress regimes during the Early Cretaceous period, which is plausible considering the debated age of the opening of the Amerasia Basin. This may indicate that the stress field at the time of the emplacement of these intrusions was markedly different and thus may represent a potentially short-lived departure from the ambient stress field. The radiating pattern of the HALIP dykes has been interpreted to reflect a mantle plume (Buchan & Ernst 2006). We suggest that the deviation in the orientation of the Cretaceous dyke swarms from the present stress field is consistent with a relatively short-lived sub-lithospheric pressure, although we are unable to draw any diagnostic conclusions about the geodynamic mechanism behind this observation.

Nearly all Late Cretaceous extensional structures and dykes are in alignment with the present day stress field, including north and NE Greenland and the adjacent Alpha Ridge. The mapped normal faults in the Laptev Sea Rift experienced rifting from the Late Cretaceous to Early Cenozoic and again in the Late Neogene. The mapped rift systems are generally in very good alignment with the geopotential stress field. A set of Permo-Triassic dykes on Bel'Kov Island in this area are also emplaced in the same direction, but these dykes are suggested to be rotated from a position as a northern continuation of the Uralides, close to Severnaya Zemlya (Pease 2011). The passive margins of Baffin Bay, the North Atlantic and the Eurasia Basin may represent the palaeostress field at the time of continental break-up from the Paleocene and Eocene (Fig. 6, red) and are also aligned with the present day stress field. Break-up in the Fram Strait and Knipovich Ridge region, however, do not show a coincident orientation.

Cenozoic extensional structures are distributed over a large part of the eastern Russian Arctic margin and largely coincide with the computed geopotential stress field (Fig. 6, magenta). As discussed earlier, the Laptev Sea Rift has experienced extension in the same orientation since the Late Cretaceous, thus the stress field in this region is assumed not to have changed significantly, despite the onset of seafloor spreading along the Gakkel Ridge and the formation of a fracture zone along the Laptev shelf area (Drachev *et al.* 2003). The Cenozoic rift system in the East Siberian Sea supposedly formed during large-scale extensional/transtensional Eocene deformation, whereas only relatively passive subsidence has been reported since the Late Cretaceous (Franke & Hinz 2009; Drachev 2011; Drachev & Shkarubo this volume, in press). A complex transtensional setting would not allow a simple interpretation of the stress regime, yet comparison with the present day geopotential stress field shows clear alignment, which could mean that the orientation of faults represent the direction of greatest compressive stress. As we

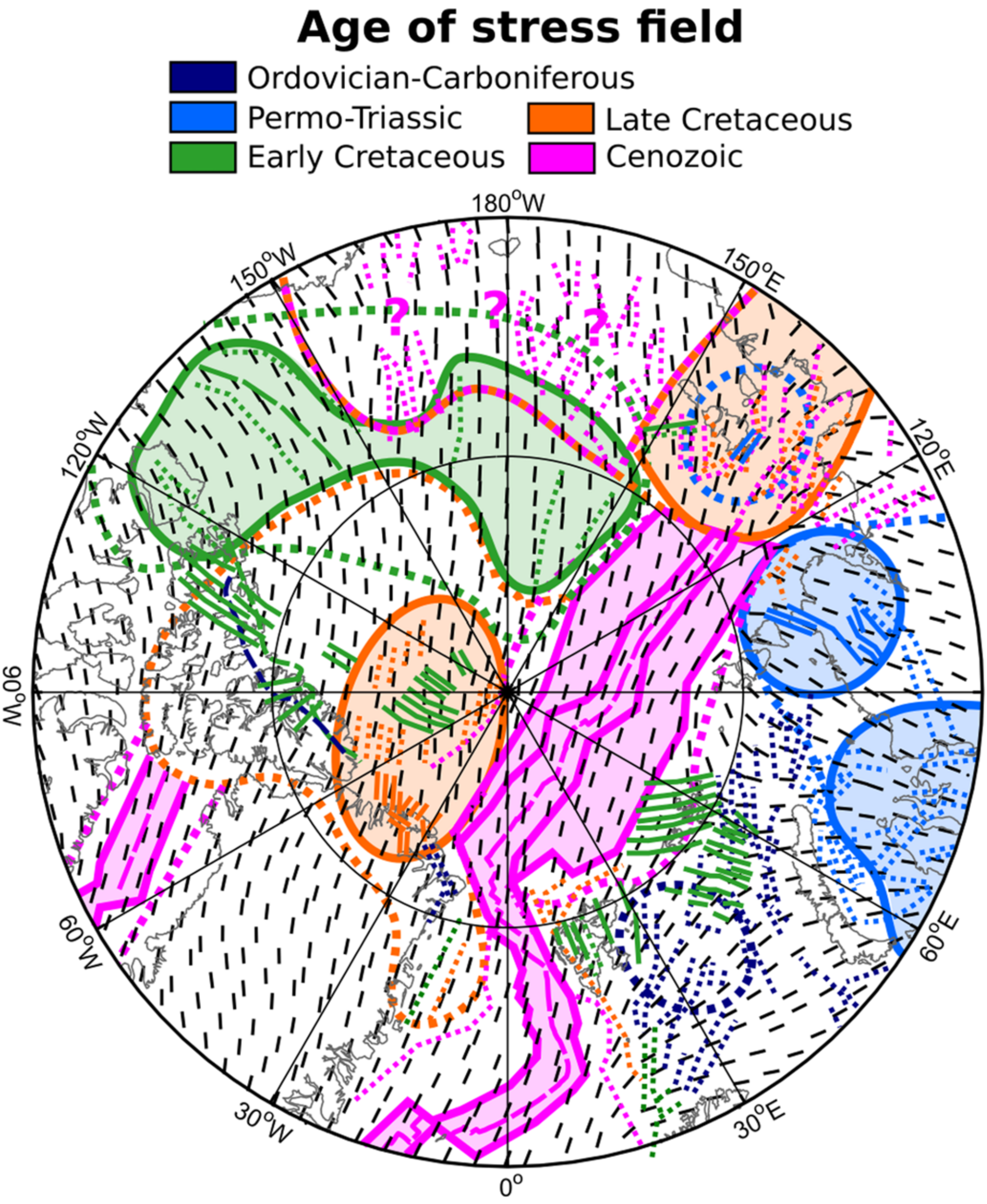

Fig. 6. Interpretation of the lithospheric stress field after comparison with palaeostress markers (dykes and rift systems). Thick solid lines are areas of observed coincidence of structures and geopotential stress field and therefore indicate when the last modification of lithospheric structure that gave rise to the geopotential stress field occurred. Thick stippled lines indicate possible extended areas, where either no extensional structure is observed or where the age is unconstrained.

cannot establish more than the alignment of faults and geopotential stress field, we will now discuss whether the faults represent the direction of most compressive stress or whether these have formed independently during a purely transtensional setting.

Discussion

As a result of the overall good agreement between the geopotential stress field and the WSM, we continue with the assumption that the computed stresses are a realistic representation of the contemporary stress field. We acknowledge that there may be errors in some regions of the calculated geopotential stress, although these are probably spatially limited and we attempt to explain them. With these caveats, the agreement or disagreement between the present day stress field and palaeostress indicators may therefore constrain when the stress field was last adjusted. This is only possible in areas where dykes or extensional basins of known age are present. However, in areas of largely homogenous stress orientations and similar geological settings, we extrapolate our conclusions over a broader area.

In cases where the present stress field deviates from the orientation of structural fabrics, we conclude that the stress field must have changed over time. By contrast, in regions where the orientations coincide, the stress field is interpreted to have remained unchanged, although we are aware that such an alignment may be coincidental. We emphasize that rifting or even the emplacement of dykes can follow inherited zones of weakness and may not entirely coincide with the actual large-scale stress field. Major tectono-thermal events have affected the High Arctic (e.g. subduction and collision zones) and their imprint may have dissipated with time. The 'passive' geopotential stress field studied here does not include such sources, but subduction has not dominated the tectonic evolution in the High Arctic since the assemblage of the Arctic part of Gondwana at *c.* 250 Ma. An exception could be the Eurekan Orogen, where subduction scenarios have been suggested (Brozena *et al.* 2003; Døssing *et al.* 2014), but it may also reflect intraplate orogenesis without a subduction component (Tessensohn & Piepjohn 2000). Northwards Palaeo-Pacific subduction beneath eastern Siberia and Alaska since *c.* 130 Ma may have had a major impact on the Early Cretaceous stress field and the subducting Pacific plate still influences the far-field stress field in the High Arctic today.

We presented evidence for Early Cretaceous dykes and graben structures on Bennett Island. Reconstruction of a rotational opening of the Amerasia Basin either along a strike-slip fault following the Lomonosov Ridge (e.g. Embry 1990) or the Alpha Ridge (Doré *et al.* 2016) would place Bennett Island and the dykes and graben proximal to northernmost Canada, Svalbard and Franz Josefs Land, and the HALIP dyke swarm (Drachev & Saunders 2003). Similarly, if the New Siberian Islands were rotated back into a position in proximity to Semeraya Zemlya as a northern continuation of the Uralides (Pease 2011), these would align with the Taimyr dyke swarm. These two regions were clearly modified by rifting of the Laptev Sea Basin at a later stage, as indicated by the stress field.

The most convincing regions in which the present day stress field coincides with palaeostress markers are given in Figure 6 and include the following. First, north Greenland and the adjacent eastern Amerasia Basin, including parts of the Alpha Ridge. Here, the lithosphere stress field seems to have remained unaltered since the Late Cretaceous (orange), whereas any effect of the stress field observed in the large radiating dyke swarms of the Early Cretaceous HALIP event (green) seems to have dissipated. The interpretation that the orientation and alkaline composition of the Late Cretaceous dyke complexes of north Greenland witnessed prolonged continental-type rifting related to the rifting of Greenland away from North America, unrelated to the Early Cretaceous HALIP (Tegner *et al.* 2011; Thórarinsson *et al.* 2015), supports this view. Even Early Cretaceous rift axes in the Amerasia Basin roughly coincide with the geopotential stress field, which emphasizes the brevity of the stress field change during the Early Cretaceous dyking event. Rifting in the Amerasia Basin may have happened independently from the emplacement of dykes in the Arctic, as suggested by the apparently very different stress regimes during both events.

Second, the stress field in the modern oceanic Eurasia Basin and parts of the North Atlantic, as well as Baffin Bay with its extinct spreading ridge, does not seem to have changed much since the Eocene. This does not, however, apply to the northernmost North Atlantic and its connection to the Arctic (Knipovich Ridge and Fram Strait), where highly complex and oblique rifting associated with the transition from the Knipovich Ridge to the Gakkel Ridge and the De Geer transform (Engen *et al.* 2008) has occurred. Break-up probably followed Caledonian (or older) inherited structures and sutures (Buiter & Torsvik 2014; Schiffer *et al.* 2015*b*), which implies that the orientation of break-up was not necessarily aligned with the large-scale tectonic stress field. This complexity could explain the overall misfit of the rift systems in the adjacent western Barents Sea margin.

Third, Late Cretaceous and Cenozoic rifting in the Laptev Sea correspond well with the recent stress field, indicating that no large-scale readjustment has occurred in this area, although seafloor spreading initiated along the Gakkel Ridge in the Eocene. Supposedly Cenozoic rifting in the East Siberian Sea is also aligned with the present day geopotential stress field, yet these rifts are thought to have formed under transtensional deformation. Permo-Triassic dykes on the New Siberian Islands show a very similar orientation, but these might be rotated as mentioned earlier, whereas the Early Cretaceous dykes on Bennett Island are not aligned. Like the HALIP dykes, this could indicate that the Early Cretaceous structures on Bennett Island were emplaced during a short-lived, transient deviation of the lithospheric stress field. The coincidence of the Permo-Triassic dykes, the Late Cretaceous rift systems and the present day stress field indicate that the ambient stress field may have existed over a long time and was only temporarily modified during a short-lived Early Cretaceous dyking event.

The stress field in the Kara Sea, Taimyr and the West Siberian Basin may have undergone final adjustment in the Triassic shortly after Siberian Trap magmatism. The data do not suggest major changes in the lithospheric stress field after the formation of the Triassic rift basins and dykes, largely due to the close alignment of the calculated stress field in these locations.

As a result of the very homogeneous stress field and a similar origin and age, we speculate that the stress field across the eastern Eurasia Basin, the Canadian Arctic Islands and north and NW Greenland may have been adjusted during the Late Cretaceous. The stress field in the central and western Amerasia Basin may have been established in the Early Cretaceous. Similarly, the eastern Russian Arctic Shelf and the region north of the Bering Strait (*c.* 180° W) may be Cenozoic in age, but given the very similar orientation of structures and stress field in the adjacent western Amerasia Basin, which has primarily Early Cretaceous structures, we speculate that the eastern Russian Arctic Shelf could also be of Early Cretaceous age.

Two regions of distinct complexity are immediately apparent. The western Barents Sea–Fram Strait–Knipovich Ridge region has a complex stress field and a complex succession of structures of different ages; the WSM coincides with neither the computed stresses nor the structures. The area east of Taimyr and west of the New Siberian Islands (*c.* 120° E) shows strong structural complexity, with a misfit between the WSM and the computed stresses, as well between structures and the stress field. Both regions are situated at the edge of the thick lithosphere and sharp LAB depth gradients, which might be one of many possible reasons for this misfit. Large gradients in LAB depth produce a large gradient in GPE and therefore have a large impact on the direction of the geopotential stress field. Stress measurements from borehole breakouts have been used in the western Barents Sea and in the Beaufort Sea and the differing depth sensitivities between these two methods may explain parts of the apparent misfit of the computed stress field and the WSM.

Summary

We present a new interpretation of the lithospheric stress field of the High Arctic at the present day and over geological history by comparing a calculated geopotential stress field with palaeostress indicators, such as magmatic dykes and extensional basins. A lithospheric density model – compiled from new sedimentary thickness, crustal thickness, dynamic topography and LAB depth models – was used to calculate the GPE and the geopotential stress field. We collected published occurrences of mafic dykes and extensional basins in the High Arctic and included new observations from Bennett Island of the De Long Islands, where Early Cretaceous dykes and an associated graben structure were recognized. We utilized these structures as palaeostress indicators and compared them with the previously computed representation of the present day stress field. We assumed that areas of matching palaeo- and present day stress directions may provide a minimum age for the last stress field configuration. Conversely, a mismatch may indicate that the stress field was subsequently reconfigured.

We conclude that, apart from the oldest sedimentary basins in the Barents Sea region and a few other exceptions, all the major rift basins appear to align with our model of contemporary geopotential stress. Furthermore, Late Cretaceous dykes in northern Greenland and Permo-Triassic dykes on Taimyr show this same alignment and may be indicative of the time of the last lithospheric modification in these areas. This is in contrast with the orientation of Early Cretaceous dykes, none of which align with the computed stress field, indicating a short-lived deviation from the ambient stress field. Early Cretaceous dykes related to the HALIP and extensional structures related to the opening of the Eurasia Basin do not show similar orientations, implying that these two events (HALIP and Amerasia Basin opening) were distinct in time.

This paper was produced during a postdoctoral fellowship of C. Schiffer, financed by the Carlsberg Foundation. Thanks go to the Circum Arctic Lithospheric Evolution (CALE) project and all active participants for many constructive discussions at excellent workshops and meetings. This study was largely motivated during CALE activities. Thanks to Nina Lebedeva-Ivanova for providing the Arctic crustal dataset. A. Schaeffer is funded by a Natural Sciences and Engineering Research Council of Canada Postdoctoral Fellowship, V. Pease is funded by the Swedish Research Council and C. Tegner is funded by the Danish National Research Foundation. We appreciate the constructive comments and suggestions from Tony Doré and an anonymous reviewer, which helped to improve the paper.

References

Altenbernd, T., Jokat, W., Heyde, I. & Damm, V. 2015. Geophysical evidence for the extent of crustal types and the type of margin along a profile in the northeastern Baffin Bay. *Journal of Geophysical*

Research: Solid Earth, **120**, JB012307, https://doi.org/10.1002/2015JB012307

Alvey, A., Gaina, C., Kusznir, N.J. & Torsvik, T.H. 2008. Integrated crustal thickness mapping and plate reconstructions for the high Arctic. *Earth and Planetary Science Letters*, **274**, 310–321, https://doi.org/10.1016/j.epsl.2008.07.036

Anfinson, O.A., Leier, A.L., Gaschnig, R., Embry, A.F. & Dewing, K. 2012. U–Pb and Hf isotopic data from Franklinian Basin strata: insights into the nature of Crockerland and the timing of accretion, Canadian Arctic Islands. *Canadian Journal of Earth Sciences*, **49**, 1316–1328, https://doi.org/10.1139/e2012-067

Anudu, G.K., Stephenson, R.A., Macdonald, D.I.M. & Oakey, G.N. 2016. Geological features of the northeastern Canadian Arctic margin (Canada) revealed from analysis of potential field data. *Tectonophysics*, https://doi.org/10.1016/j.tecto.2016.03.025

Artemieva, I.M. 2009. The continental lithosphere: reconciling thermal, seismic, and petrologic data. *Lithos*, **109**, 23–46, https://doi.org/10.1016/j.lithos.2008.09.015

Artemieva, I.M. & Thybo, H. 2013. EUNAseis: a seismic model for Moho and crustal structure in Europe, Greenland, and the North Atlantic region. *Tectonophysics*, **609**, 97–153, https://doi.org/10.1016/j.tecto.2013.08.004

Beranek, L.P., Mortensen, J.K., Lane, L.S., Allen, T.L., Fraser, T.A., Hadlari, T. & Zantvoort, W.G. 2010. Detrital zircon geochronology of the western Ellesmerian clastic wedge, northwestern Canada: insights on Arctic tectonics and the evolution of the northern Cordilleran miogeocline. *Geological Society of America Bulletin*, **122**, 1899–1911, https://doi.org/10.1130/B30120.1

Bird, P. & Piper, K. 1980. Plane-stress finite-element models of tectonic flow in southern California. *Physics of the Earth and Planetary Interiors*, **21**, 158–175, https://doi.org/10.1016/0031-9201(80)90067-9

Bouhifd, M.A., Andrault, D., Fiquet, G. & Richet, P. 1996. Thermal expansion of forsterite up to the melting point. *Geophysical Research Letters*, **23**, 1143–1146, https://doi.org/10.1029/96GL01118

Brozena, J.M., Childers, V.A., Lawver, L.A., Gahagan, L.M., Forsberg, R., Faleide, J.I. & Eldholm, O. 2003. New aerogeophysical study of the Eurasia Basin and Lomonosov Ridge: implications for basin development. *Geology*, **31**, 825–828, https://doi.org/10.1130/G19528.1

Brumley, K. 2010. *Tectonic geomorphology of the Chukchi Borderland: constraint for tectonic reconstruction models*. MS thesis, University of Alaska.

Burgess, S.D. & Bowring, S.A. 2014. High-precision geochronology conforms voluminous magmatism before, during, and after Earth's most severe mass extinction. *Sci. Adv.*, **1**, e1500470, https://doi.org/10.1126/sciadv.1500470

Buchan, K.L. & Ernst, R.E. 2006. The High Arctic Large Igneous Province (HALIP): evidence for an associated giant radiating dyke swarm, http://www.largeigneousprovinces.org/06apr

Buiter, S.J.H. & Torsvik, T.H. 2014. A review of Wilson cycle plate margins: a role for mantle plumes in continental break-up along sutures? *Gondwana Research*, **26**, 627–653, https://doi.org/10.1016/j.gr.2014.02.007

Chalmers, J.A. & Pulvertaft, T.C.R. 2001. Development of the continental margins of the Labrador Sea: a review. *In*: Wilson, R.C.L., Whitmarsh, R.B., Taylor, B. & Froitzheim, M. (eds) *Non-Volcanic Rifting of Continental Margins: A Comparison of Evidence from Land and Sea*. Geological Society, London, Special Publications, **187**, 77–105, https://doi.org/10.1144/GSL.SP.2001.187.01.05

Chian, D., Jackson, H.R. *et al.* 2016. Distribution of crustal types in Canada Basin, Arctic Ocean. *Tectonophysics*, **691**, 8–30.

Cocks, L.R.M. & Torsvik, T.H. 2007. Siberia, the wandering northern terrane, and its changing geography through the Palaeozoic. *Earth Science Reviews*, **82**, 29–74, https://doi.org/10.1016/j.earscirev.2007.02.001

Conrad, C.P. & Lithgow-Bertelloni, C. 2006. Influence of continental roots and asthenosphere on plate-mantle coupling. *Geophysical Research Letters*, **33**, L05312, https://doi.org/10.1029/2005GL025621

Corfu, F., Polteau, S., Planke, S., Faleide, J.I., Svensen, H., Zayoncheck, A. & Stolbov, N. 2013. U–Pb geochronology of Cretaceous magmatism on Svalbard and Franz Josef Land, Barents Sea Large Igneous Province. *Geological Magazine*, **150**, 1127–1135, https://doi.org/10.1017/S0016756813000162

Curtis, M., Lopez-Mir, B., Scott, R. & Howard, J.P. In press. Early Mesozoic sinistral transpression along the Pai-Khoi – Novaya Zemlya fold and-thrust belt, Russia. *In*: Pease, V. & Coakley, B. (eds) *Circum-Arctic Lithosphere Evolution*. Geological Society, London, Special Publications, **460**, https://doi.org/10.1144/SP460.2

Danukalova, M.K., Kuzmichev, A.B. & Aristov, V.A. 2014. Upper Devonian depositional system of Bel'kov Island (New Siberian Islands): an intracontinental rift or a continental margin? *Geotectonics*, **48**, 390–412, https://doi.org/10.1134/S0016852114050021

Dibner, V.D. (ed.) 1998. Geology of Franz Josef Land, Norsk Polarinstitut, Oslo, Meddelelse, 146.

Doré, A.G., Lundin, E.R., Gibbons, A., Sømme, T.O. & Tørudbakken, B.O. 2016. Transform margins of the Arctic: a synthesis and re-evaluation. *In*: Nemčok, M., Rybár, S., Sinha, S.T., Hermeston, S.A. & Ledvényiová, L.A. (eds) *Transform Margins: Development, Controls and Petroleum Systems*. Geological Society, London, Special Publications, **431**, 63–94, https://doi.org/10.1144/SP431.8

Døssing, A., Hopper, J.R., Olesen, A.V., Rasmussen, T.M. & Halpenny, J. 2013*a*. New aero-gravity results from the Arctic: linking the latest Cretaceous–early Cenozoic plate kinematics of the North Atlantic and Arctic Ocean. *Geochemistry, Geophysics, Geosystems*, **14**, 4044–4065, https://doi.org/10.1002/ggge.20253

Døssing, A., Jackson, H.R., Matzka, J., Einarsson, I., Rasmussen, T.M., Olesen, A.V. & Brozena, J.M. 2013*b*. On the origin of the Amerasia Basin and the High Arctic Large Igneous Province – results of new aeromagnetic data. *Earth and Planetary Science Letters*, **363**, 219–230, https://doi.org/10.1016/j.epsl.2012.12.013

Døssing, A., Hansen, T.M., Olesen, A.V., Hopper, J.R. & Funck, T. 2014. Gravity inversion predicts the nature of the Amundsen Basin and its continental borderlands near Greenland. *Earth and Planetary Science Letters*, **408**, 132–145, https://doi.org/10.1016/j.epsl.2014.10.011

Drachev, S. & Saunders, A. 2003. The Early Cretaceous Arctic LIP: its geodynamic setting and implications for Canada Basin opening. *In: Proceedings of the Fourth International Conference on Arctic Margins, OCS Study, MMS 2006-003*, 30 September–3 October 2003, Anchorage, AK, USA, 216–223.

Drachev, S.S. 2011. Tectonic setting, structure and petroleum geology of the Siberian Arctic offshore sedimentary basins. *In*: Spencer, A.M., Embry, A.F., Gautier, D.L., Stoupakova, A.V. & Sørensen, K. (eds) *Arctic Petroleum Geology*. Geological Society, London, Memoirs, **35**, 369–394, https://doi.org/10.1144/M35.25

Drachev, S.S. 2016. Fold belts and sedimentary basins of the Eurasian Arctic. *Arktos*, **2**, 1–30, https://doi.org/10.1007/s41063-015-0014-8

Drachev, S.S. & Shkarubo, S. In press. Tectonics of the Laptev Shelf, Siberian Arctic. *In*: Pease, V. & Coakley, B. (eds) *Circum-Arctic Lithosphere Evolution*. Geological Society, London, Special Publications, **460**, https://doi.org/10.1144/SP460.15

Drachev, S.S., Kaul, N. & Beliaev, V.N. 2003. Eurasia spreading basin to Laptev Shelf transition: structural pattern and heat flow. *Geophysical Journal International*, **152**, 688–698, https://doi.org/10.1046/j.1365-246X.2003.01882.x

Drachev, S.S., Malyshev, N.A. & Nikishin, A.M. 2010. Tectonic history and petroleum geology of the Russian Arctic Shelves: an overview. *In*: Vining, B.A. & Pickering, S.C. (eds) *Petroleum Geology: From Mature Basins to New Frontiers – Proceedings of the 7th Petroleum Geology Conference*. Geological Society, London, 591–619, https://doi.org/10.1144/0070591

Dutro, J.T. 1981. Geology of Alaska bordering the Arctic Ocean. *In*: Nairn, A.E.M., Churkin, M. & Stehli, F.G. (eds) *The Arctic Ocean*. Springer, New York, 21–36.

Eaton, D.W., Darbyshire, F., Evans, R.L., Grütter, H., Jones, A.G. & Yuan, X. 2009. The elusive lithosphere–asthenosphere boundary (LAB) beneath cratons. *Lithos*, **109**, 1–22, https://doi.org/10.1016/j.lithos.2008.05.009

Ebbing, J., England, R.W., Korja, T., Lauritsen, T., Olesen, O., Stratford, W. & Weidle, C. 2012. Structure of the Scandes lithosphere from surface to depth. *Tectonophysics*, **536–537**, 1–24, https://doi.org/10.1016/j.tecto.2012.02.016

Embry, A.F. 1990. Geological and geophysical evidence in support of the hypothesis of anticlockwise rotation of northern Alaska. *Marine Geology*, **93**, 317–329, https://doi.org/10.1016/0025-3227(90)90090-7

Embry, A.F. 1991. Mesozoic history of the Arctic Islands. *In*: Trettin, H.P. (ed.) *Geology of the Innuitian Orogen and Arctic Platform of Canada and Greenland*. Geological Survey of Canada, Geology of Canada, **3**, 371–433.

Embry, A. & Beauchamp, B. 2008. Sverdrup Basin. *In*: Andrew, D.M. (ed.) *Sedimentary Basins of the World: the Sedimentary Basins of the United States and Canada*. Elsevier, Amsterdam, 451–471.

Embry, A.F. & Dixon, J. 1990. The breakup unconformity of the Amerasia Basin, Arctic Ocean: evidence from Arctic Canada. *Geological Society of America Bulletin*, **102**, 1526–1534, https://doi.org/10.1130/0016-7606(1990)1022.3.CO;2

Engen, Ø., Eldholm, O. & Bungum, H. 2003. The Arctic plate boundary. *Journal of Geophysical Research: Solid Earth*, **108**, https://doi.org/10.1029/2002JB001809

Engen, Ø., Faleide, J.I. & Dyreng, T.K. 2008. Opening of the Fram Strait gateway: a review of plate tectonic constraints. *Tectonophysics*, **450**, 51–69, https://doi.org/10.1016/j.tecto.2008.01.002

England, P. & Houseman, G. 1986. Finite strain calculations of continental deformation: 2. Comparison with the India–Asia collision zone. *Journal of Geophysical Research: Solid Earth*, **91**, 3664–3676, https://doi.org/10.1029/JB091iB03p03664

England, P. & McKenzie, D. 1982. A thin viscous sheet model for continental deformation. *Geophysical Journal of the Royal Astronomical Society*, **70**, 295–321, https://doi.org/10.1111/j.1365-246X.1982.tb04969.x

Estrada, S. & Henjes-Kunst, F. 2013. ^{40}Ar–^{39}Ar and U–Pb dating of Cretaceous continental rift-related magmatism on the northeast Canadian Arctic margin [in German]. *Zeitschrift Deutsche Gesellschaft für Geowissenschaften*, **164**, 107–130, https://doi.org/10.1127/1860-1804/2013/0005

Estrada, S., Henjes-Kunst, F., Melcher, F. & Tessensohn, F. 2010. Paleocene alkaline volcanism in the Nares Strait region: evidence from volcanic pebbles. *International Journal of Earth Sciences*, **99**, 863–890, https://doi.org/10.1007/s00531-009-0432-6

Evenchick, C.A., Davis, W.J., Bédard, J.H., Hayward, N. & Friedman, R.M. 2015. Evidence for protracted High Arctic large igneous province magmatism in the central Sverdrup Basin from stratigraphy, geochronology, and paleodepths of saucer-shaped sills. *Geological Society of America Bulletin*, B31190.1, https://doi.org/10.1130/B31190.1

Faleide, I.J., Pease, V. *et al.* In review. Lithospheric transects across the Barents and Kara shelves, and tectonic implications. *In*: Pease, V. & Coakley, B. (eds) *Circum-Arctic Lithosphere Evolution*. Geological Society, London, Special Publications, **460**.

Faleide, J.I., Tsikalas, F. *et al.* 2008. Structure and evolution of the continental margin off Norway and the Barents Sea. *Episodes*, **31**, 82–91.

Fischer, K.M., Ford, H.A., Abt, D.L. & Rychert, C.A. 2010. The lithosphere–asthenosphere boundary. *Annual Review of Earth and Planetary Sciences*, **38**, 551–575, https://doi.org/10.1146/annurev-earth-040809-152438

Flesch, L.M., Haines, A.J. & Holt, W.E. 2001. Dynamics of the India–Eurasia collision zone. *Journal of Geophysical Research: Solid Earth*, **106**, 16435–16460, https://doi.org/10.1029/2001JB000208

Franke, D. & Hinz, K. 2009. Geology of the Shelves surrounding the New Siberian Islands, Russian Arctic.

In: Stone, D.B., Fujita, K., Layer, P.L., Miller, E.L., Prokopiev, A.V. & Toro, J. (eds) *Geology, Geophysics and Tectonics of Northeastern Russia: a Tribute to Leonid Parfenov*. European Geosciences Union, Stephan Mueller Special Publication Series, **4**. Copernicus, Göttingen, 35–44.

Franke, D., Hinz, K. & Oncken, O. 2001. The Laptev Sea rift. *Marine and Petroleum Geology*, **18**, 1083–1127, https://doi.org/10.1016/S0264-8172(01)00041-1

Franke, D., Hinz, K. & Reichert, C. 2004. Geology of the East Siberian Sea, Russian Arctic, from seismic images: structures, evolution, and implications for the evolution of the Arctic Ocean Basin: geology of the East Siberian Shelf. *Journal of Geophysical Research: Solid Earth*, **109**, https://doi.org/10.1029/2003JB002687

Funck, T., Jackson, H.R. & Shimeld, J. 2011. The crustal structure of the Alpha Ridge at the transition to the Canadian polar margin: results from a seismic refraction experiment. *Journal of Geophysical Research: Solid Earth*, **116**, B12101, https://doi.org/10.1029/2011JB008411

Funck, T., Gohl, K., Damm, V. & Heyde, I. 2012. Tectonic evolution of southern Baffin Bay and Davis Strait: results from a seismic refraction transect between Canada and Greenland. *Journal of Geophysical Research: Solid Earth*, **117**, https://doi.org/10.1029/2011JB009110

Gaina, C., Werner, S.C., Saltus, R. & Maus, S. 2011. Circum-Arctic mapping project: new magnetic and gravity anomaly maps of the Arctic. *In*: Spencer, A.M., Embry, A.F., Gautier, D.L., Stoupakova, A.V. & Sørensen, K. (eds) *Arctic Petroleum Geology*. Geological Society, London, Memoirs, **35**, 39–48, https://doi.org/10.1144/M35.3

Gaina, C., Medvedev, S., Torsvik, T.H., Koulakov, I. & Werner, S.C. 2013. 4D Arctic: a glimpse into the structure and evolution of the Arctic in the light of new geophysical maps, plate tectonics and tomographic models. *Surveys in Geophysics*, **35**, 1095–1122, https://doi.org/10.1007/s10712-013-9254-y

Gaina, C., Nikishin, A.M. & Petrov, E.I. 2015. Ultraslow spreading, ridge relocation and compressional events in the East Arctic region: a link to the Eurekan orogeny? *Arktos*, **1**, 1–11, https://doi.org/10.1007/s41063-015-0006-8

Gasser, D. 2013. The Caledonides of Greenland, Svalbard and other Arctic areas: status of research and open questions. *In*: Corfu, F., Gasser, D. & Chew, D.M. (eds) *New Perspectives on the Caledonides of Scandinavia and Related Areas*. Geological Society, London, Special Publications, **390**, 93–129, https://doi.org/10.1144/SP390.17

Gee, D.G. 2015. Caledonides of Scandinavia, Greenland, and Svalbard. *In*: Elias, S.A. (ed.) *Reference Module in Earth Systems and Environmental Sciences*. Elsevier, Amsterdam.

Gee, D.G. & Pease, V. 2004. The Neoproterozoic Timanide Orogen of eastern Baltica: introduction. *In*: Gee, D.G. & Pease, V. (eds) *The Neoproterozoic Timanide Orogen of Eastern Baltica*. Geological Society, London, Memoirs, **30**, 1–3, https://doi.org/10.1144/GSL.MEM.2004.030.01.01

Gee, D.G., Fossen, H., Henriksen, N. & Higgins, A.K. 2008. From the early Paleozoic platforms of Baltica and Laurentia to the Caledonide orogen of Scandinavia and Greenland. *Episodes*, **31**, 44–51.

Gernigon, L., Blischke, A., Nasuti, A. & Sand, M. 2015. Conjugate volcanic rifted margins, sea-floor spreading and microcontinent: insights from new high-resolution aeromagnetic surveys in the Norway Basin. *Tectonics*, 2014TC003717, https://doi.org/10.1002/2014TC003717

Ghosh, A., Holt, W.E., Wen, L., Haines, A.J. & Flesch, L.M. 2008. Joint modeling of lithosphere and mantle dynamics elucidating lithosphere-mantle coupling. *Geophysical Research Letters*, **35**, L16309, https://doi.org/10.1029/2008GL034365

Glebovsky, V.Y., Kaminsky, V.D., Minakov, A.N., Merkur'ev, S.A., Childers, V.A. & Brozena, J.M. 2006. Formation of the Eurasia Basin in the Arctic Ocean as inferred from geohistorical analysis of the anomalous magnetic field. *Geotectonics*, **40**, 263–281, https://doi.org/10.1134/S001685210604 0029

Grad, M., Tiira, T. & ESC Working Group 2009. The Moho depth map of the European plate. *Geophysical Journal International*, **176**, 279–292, https://doi.org/10.1111/j.1365-246X.2008.03919.x

Grantz, A., Clark, D.L. *et al.* 1998. Phanerozoic stratigraphy of Northwind Ridge, magnetic anomalies in the Canada basin, and the geometry and timing of rifting in the Amerasia basin, Arctic Ocean. *Geological Society of America Bulletin*, **110**, 801–820, https://doi.org/10.1130/0016-7606(1998)1102.3.CO;2

Grantz, A., Pease, V.L., Willard, D.A., Phillips, R.L. & Clark, D.L. 2001. Bedrock cores from 89° North: implications for the geologic framework and Neogene paleoceanography of Lomonosov Ridge and a tie to the Barents shelf. *Geological Society of America Bulletin*, **113**, 1272–1281, https://doi.org/10.1130/0016-7606(2001)1132.0.CO;2

Grantz, A., Hart, P.E. & Childers, V.A. 2011. Geology and tectonic development of the Amerasia and Canada Basins, Arctic Ocean. *In*: Spencer, A.M., Embry, A.F., Gautier, D.L., Stoupakova, A.V. & Sørensen, K. (eds) *Arctic Petroleum Geology*. Geological Society, London, Memoirs, **35**, 771–799, https://doi.org/10.1144/M35.50

Gudlaugsson, S.T., Faleide, J.I., Johansen, S.E. & Breivik, A.J. 1998. Late Palaeozoic structural development of the south-western Barents Sea. *Marine and Petroleum Geology*, **15**, 73–102, https://doi.org/10.1016/S0264-8172(97)00048-2

Håkansson, E. & Stemmerik, L. 1989. Wandel Sea basin – a new synthesis of the late Paleozoic to Tertiary accumulation in North Greenland. *Geology*, **17**, 683–686, https://doi.org/10.1130/0091-7613(1989)0172.3.CO;2

Heidbach, O., Tingay, M., Barth, A., Reinecker, J., Kurfess, D. & Müller, B. 2010. Global crustal stress pattern based on the World Stress Map database release 2008. *Tectonophysics*, **482**, 3–15, https://doi.org/10.1016/j.tecto.2009.07.023

Henriksen, E., Ryseth, A.E., Larssen, G.B., Heide, T., Rønning, K., Sollid, K. & Stoupakova, A.V. 2011. Tectonostratigraphy of the greater Barents Sea: implications for petroleum systems. *In*: Spencer, A.M., Embry, A.F., Gautier, D.L., Stoupakova, A.V. & Sørensen, K. (eds) *Arctic Petroleum Geology*. Geological Society, London, Memoirs, **35**, 163–195, https://doi.org/10.1144/M35.10

Hosseinpour, M., Müller, R.D., Williams, S.E. & Whittaker, J.M. 2013. Full-fit reconstruction of the Labrador Sea and Baffin Bay. *Solid Earth*, **4**, 461–479, https://doi.org/10.5194/se-4-461-2013

Inger, S., Scott, R.A. & Golionko, B.G. 1999. Tectonic evolution of the Taimyr Peninsula, northern Russia: implications for Arctic continental assembly. *Journal of the Geological Society, London*, **156**, 1069–1072, https://doi.org/10.1144/gsjgs.156.6.1069

Ivanov, A.V., He, H., Yan, L., Ryabov, V.V., Shevko, A.Y., Palesskii, S.V. & Nikolaeva, I.V. 2013. Siberian Traps large igneous province: evidence for two flood basalt pulses around the Permo-Triassic boundary and in the Middle Triassic, and contemporaneous granitic magmatism. *Earth-Science Reviews*, **122**, 58–76, https://doi.org/10.1016/j.earscirev.2013.04.001

Ivanova, N.M., Sakulina, T.S., Belyaev, I.V., Matveev, Y.I. & Roslov, Y.V. 2011. Depth model of the Barents and Kara seas according to geophysical surveys results. *In*: Spencer, A.M., Embry, A.F., Gautier, D.L., Stoupakova, A.V. & Sørensen, K. (eds) *Arctic Petroleum Geology*. Geological Society, London, Memoirs, **35**, 209–221, https://doi.org/10.1144/M35.12

Jackson, H.R., Dahl-Jensen, T. & LORITA Working Group 2010. Sedimentary and crustal structure from the Ellesmere Island and Greenland continental shelves onto the Lomonosov Ridge, Arctic Ocean. *Geophysical Journal International*, **182**, 11–35, https://doi.org/10.1111/j.1365-246X.2010.04604.x

Jokat, W. 2003. Seismic investigations along the western sector of Alpha Ridge, Central Arctic Ocean. *Geophysical Journal International*, **152**, 185–201, https://doi.org/10.1046/j.1365-246X.2003.01839.x

Jokat, W., Uenzelmann-Neben, G., Kristoffersen, Y. & Rasmussen, T.M. 1992. Lomonosov Ridge – a double-sided continental margin. *Geology*, **20**, 887–890, https://doi.org/10.1130/0091-7613(1992)0202.3.CO;2

Kennett, B.L.N., Engdahl, E.R. & Buland, R. 1995. Constraints on seismic velocities in the Earth from travel times. *Geophysical Journal International*, **122**, 108–124, https://doi.org/10.1111/j.1365-246X.1995.tb03540.x

Klimenko, S.S., Anischenko, L.A. & Antoshkina, A.I. 2011. The Timan–Pechora sedimentary basin: Palaeozoic reef formations and petroleum systems. *In*: Spencer, A.M., Embry, A.F., Gautier, D.L., Stoupakova, A.V. & Sørensen, K. (eds) *Arctic Petroleum Geology*. Geological Society, London, Memoirs, **35**, 223–236, https://doi.org/10.1144/M35.13

Klitzke, P., Faleide, J.I., Scheck-Wenderoth, M. & Sippel, J. 2015. A lithosphere-scale structural model of the Barents Sea and Kara Sea region. *Solid Earth*, **6**, 153–172, https://doi.org/10.5194/se-6-153-2015

Kravchinsky, V.A., Cogné, J.-P., Harbert, W.P. & Kuzmin, M.I. 2002. Evolution of the Mongol–Okhotsk Ocean as constrained by new palaeomagnetic data from the Mongol–Okhotsk suture zone, Siberia. *Geophysical Journal International*, **148**, 34–57, https://doi.org/10.1046/j.1365-246x.2002.01557.x

Kuzmichev, A.B. & Pease, V.L. 2007. Siberian trap magmatism on the New Siberian Islands: constraints for Arctic Mesozoic plate tectonic reconstructions. *Journal of the Geological Society, London*, **164**, 959–968, https://doi.org/10.1144/0016-76492006-090

Lane, L.S. 1997. Canada Basin, Arctic Ocean: evidence against a rotational origin. *Tectonics*, **16**, 363–387, https://doi.org/10.1029/97TC00432

Laske, G., Masters, G., Ma, Z. & Pasyanos, M. 2013. Update on CRUST1.0 – a 1-degree global model of Earth's crust. *In*: *EGU General Assembly Conference Abstracts*, 15, 20132658abstrEGU, 7–12 April, Vienna, Austria.

Lawver, L.A., Gahagan, L.M. & Norton, I. 2011. Palaeogeographic and tectonic evolution of the Arctic region during the Palaeozoic. *In*: Spencer, A.M., Embry, A.F., Gautier, D.L., Stoupakova, A.V. & Sørensen, K. (eds) *Arctic Petroleum Geology*. Geological Society, London, Memoirs, **35**, 61–77, https://doi.org/10.1144/M35.5

Lebedev, S. & Van Der Hilst, R.D. 2008. Global upper-mantle tomography with the automated multimode inversion of surface and S-wave forms. *Geophysical Journal International*, **173**, 505–518, https://doi.org/10.1111/j.1365-246X.2008.03721.x

Lebedeva-Ivanova, N.N., Zamansky, Y.Y., Langinen, A.E. & Sorokin, M.Y. 2006. Seismic profiling across the Mendeleev Ridge at 82°N: evidence of continental crust. *Geophysical Journal International*, **165**, 527–544, https://doi.org/10.1111/j.1365-246X.2006.02859.x

Lebedeva-Ivanova, N.N., Gee, D.G. & Sergeyev, M.B. 2011. Crustal structure of the East Siberian continental margin, Podvodnikov and Makarov basins, based on refraction seismic data (TransArctic 1989–1991). *In*: Spencer, A.M., Embry, A.F., Gautier, D.L., Stoupakova, A.V. & Sørensen, K. (eds) *Arctic Petroleum Geology*. *Geological Society, London, Memoirs*, **35**, 395–411, https://doi.org/10.1144/M35.26

Lebedeva-Ivanova, N.N., Gaina, C., Minakov, A. & Kashubin, S. 2015. A new model of the Arctic crustal thickness from 3D gravity inversion. *Abstract presented at the AGU Fall Meeting*, 14–18 December 2015, San Francisco, USA.

Lebedeva-Ivanova, N., Gaina, C., Minakov, A. & Kashubin, S. In review. ArcCRUST: arctic Moho and crustal thickness from 3D gravity inversion. *Earth and Planetary Science Letters*.

Lemieux, Y., Hadlari, T. & Simonetti, A. 2011. Detrital zircon geochronology and provenance of Devono-Mississippian strata in the northern Canadian Cordilleran miogeocline. *Canadian Journal of Earth Sciences*, **48**, 515–541, https://doi.org/10.1139/E10-056

Leslie, A.G., Smith, M. & Scoper, N.J. 2008. Laurentian margin evolution and the Caledonian orogeny – a template for Scotland and East Greenland. *In*: *The Greenland Caledonides*. Geological Society of America, Memoirs, **20**.

Li, L., Stephenson, R. & Clift, P.D. 2016. The Canada Basin compared to the southwest South China

Sea: two marginal ocean basins with hyper-extended continent–ocean transitions. *Tectonophysics*, https://doi.org/10.1016/j.tecto.2016.02.042

Lorenz, H., Gee, D.G., Larionov, A.N. & Majka, J. 2012. The Grenville–Sveconorwegian orogen in the high Arctic. *Geological Magazine*, **149**, 875–891, https://doi.org/10.1017/S0016756811001130

Maher, H.D. 2001. Manifestations of the Cretaceous High Arctic Large Igneous Province in Svalbard. *Journal of Geology*, **109**, 91–104, https://doi.org/10.1086/317960

Marello, L., Ebbing, J. & Gernigon, L. 2013. Basement inhomogeneities and crustal setting in the Barents Sea from a combined 3D gravity and magnetic model. *Geophysical Journal International*, **193**, 557–584, https://doi.org/10.1093/gji/ggt018

McKenzie, D. & Bickle, M.J. 1988. The volume and composition of melt generated by extension of the lithosphere. *Journal of Petrology*, **29**, 625–679, https://doi.org/10.1093/petrology/29.3.625

McKenzie, D., Jackson, J. & Priestley, K. 2005. Thermal structure of oceanic and continental lithosphere. *Earth and Planetary Science Letters*, **233**, 337–349, https://doi.org/10.1016/j.epsl.2005.02.005

Minakov, A., Faleide, J.I., Glebovsky, V.Y. & Mjelde, R. 2012. Structure and evolution of the northern Barents–Kara Sea continental margin from integrated analysis of potential fields, bathymetry and sparse seismic data. *Geophysical Journal International*, **188**, 79–102, https://doi.org/10.1111/j.1365-246X.2011.05258.x

Morozov, A.F., Petrov, O.V. & *et al.* 2013. New geological data are confirming continental origin of the central Arctic rises. *Expedition*, 2012, **53**, 24–55.

Mosar, J., Lewis, G. & Torsvik, T. 2002. North Atlantic sea-floor spreading rates: implications for the Tertiary development of inversion structures of the Norwegian–Greenland Sea. *Journal of the Geological Society, London*, **159**, 503–515, https://doi.org/10.1144/0016-764901-135

Müller, R.D., Sdrolias, M., Gaina, C. & Roest, W.R. 2008. Age, spreading rates, and spreading asymmetry of the world's ocean crust. *Geochemistry, Geophysics, Geosystems*, **9**, Q04006, https://doi.org/10.1029/2007GC001743

Nielsen, S.B., Stephenson, R. & Thomsen, E. 2007. Dynamics of Mid-Palaeocene North Atlantic rifting linked with European intra-plate deformations. *Nature*, **450**, 1071–1074, https://doi.org/10.1038/nature06379

Nielsen, S.B., Stephenson, R. & Schiffer, C. 2014. Deep controls on intraplate basin inversion. *In*: Talwani, P. (ed.) *Intraplate Earthquakes*, Cambridge University Press, Cambridge, 257–274.

Nikishin, A.M., Ziegler, P.A. *et al.* 1996. Late Precambrian to Triassic history of the East European Craton: dynamics of sedimentary basin evolution. *Tectonophysics*, **268**, 23–63, https://doi.org/10.1016/S0040-1951(96)00228-4

Nikishin, A.M., Sobornov, K.O., Prokopiev, A.V. & Frolov, S.V. 2010. Tectonic evolution of the Siberian Platform during the Vendian and Phanerozoic. *Moscow University Geology Bulletin*, **65**, 1–16, https://doi.org/10.3103/S0145875210010011

Nikishin, A.M., Malyshev, N.A. & Petrov, E.I. 2014. Geological structure and history of the Arctic Ocean, EAGE Publications, The Netherlands.

Oakey, G.N. & Chalmers, J.A. 2012. A new model for the Paleogene motion of Greenland relative to North America: plate reconstructions of the Davis Strait and Nares Strait regions between Canada and Greenland. *Journal of Geophysical Research*, **117**, https://doi.org/10.1029/2011JB008942

Oakey, G.N. & Stephenson, R. 2008. Crustal structure of the Innuitian region of Arctic Canada and Greenland from gravity modelling: implications for the Palaeogene Eurekan orogen. *Geophysical Journal International*, **173**, 1039–1063, https://doi.org/10.1111/j.1365-246X.2008.03784.x

Okulitch, A.V. & Trettin, H.P. 1991. Late Cretaceous–Early Tertiary deformation, Arctic Islands. *In*: Trettin, H.P. (ed.) *Geology of the Innuitian Orogen and Arctic Platform of Canada and Greenland*. Geological Survey of Canada, Geology of Canada, **3**, 467–485.

Olesen, O., Brönner, M. *et al.* 2010. New aeromagnetic and gravity compilations from Norway and adjacent areas: methods and applications. *In*: Vining, B.A. & Pickering, S.C. (eds) *Petroleum Geology: From Mature Basins to New Frontiers – Proceedings of the 7th Petroleum Geology Conference*. Geological Society, London, 559–586, https://doi.org/10.1144/0070559

Otto, S.C. & Bailey, R.J. 1995. Tectonic evolution of the northern Ural Orogen. *Journal of the Geological Society, London*, **152**, 903–906, https://doi.org/10.1144/GSL.JGS.1995.152.01.03

Pease, V. 2011. Eurasian orogens and Arctic tectonics: an overview. *In*: Spencer, A.M., Embry, A.F., Gautier, D.L., Stoupakova, A.V. & Sørensen, K. (eds) *Arctic Petroleum Geology*. Geological Society, London, Memoirs, **35**, 311–324, https://doi.org/10.1144/M35.20

Pease, V. & Nobre Silva, I. 2015. Age and geochemistry of Cretaceous basalts from Axel Heiberg, Canada. *In*: Smelror, M. (ed.) *7th International Conference on Arctic Margins – ICAM 2015* (Abstracts), 2–5 June 2015, Trondheim, Norway.

Pease, V. & Scott, R.A. 2009. Crustal affinities in the Arctic Uralides, northern Russia: significance of detrital zircon ages from Neoproterozoic and Palaeozoic sediments in Novaya Zemlya and Taimyr. *Journal of the Geological Society, London*, **166**, 517–527, https://doi.org/10.1144/0016-76492008-093

Pease, V. & Vernikovsky, V. 2000. The tectonomagmatic evolution of the Taimyr peninsula: further constraints from new ion-microprobe data. *Polarforschung*, **68**, 171–178.

Pease, V., Drachev, S., Stephenson, R. & Zhang, X. 2014. Arctic lithosphere – a review. *Tectonophysics*, **628**, 1–25, https://doi.org/10.1016/j.tecto.2014.05.033

Petrov, O., Morozov, A. *et al.* 2016. Crustal structure and tectonic model of the Arctic region. *Earth-Science Reviews*, **154**, 29–71, https://doi.org/10.1016/j.earscirev.2015.11.013

Piepjohn, K. & von Gosen, W. In press. A structural transect through Ellesmere Island (Canadian Arctic): superimposed Palaeozoic Ellesmerian and Cenozoic Eurekan deformations. *In*: Pease, V. & Coakley, B. (eds) *Circum-Arctic Lithosphere Evolution*.

Geological Society, London, Special Publications, **460**, https://doi.org/10.1144/SP460.5

Piepjohn, K., von Gosen, W. & Tessensohn, F. 2016. The Eurekan deformation in the Arctic: an outline. *Journal of the Geological Society, London*, **173**, 1007–1024, https://doi.org/10.1144/jgs2016-081

Polteau, S., Hendriks, B.W.H. *et al.* 2016. The Early Cretaceous Barents Sea sill complex: distribution, $^{40}Ar/^{39}Ar$ geochronology, and implications for carbon gas formation. *Palaeogeography, Palaeoclimatology, Palaeoecology*, **441**, 83–95, https://doi.org/10.1016/j.palaeo.2015.07.007

Poselov, V.A., Verba, V.V. & Zholondz, S.M. 2007. Typification of the Earth's crust of Central Arctic Uplifts in the Arctic Ocean. *Geotectonics*, **41**, 296–305, https://doi.org/10.1134/S0016852107040036

Reichow, M.K., Saunders, A.D., White, R.V., Pringle, M.S., Al'Mukhamedov, A.I., Medvedev, A.I. & Kirda, N.P. 2002. $^{40}Ar/^{39}Ar$ dates from the West Siberian Basin: Siberian flood basalt province doubled. *Science*, **296**, 1846–1849, https://doi.org/10.1126/science.1071671

Reichow, M.K., Pringle, M.S. *et al.* 2009. The timing and extent of the eruption of the Siberian Traps large igneous province: implications for the end-Permian environmental crisis. *Earth and Planetary Science Letters*, **277**, 9–20, https://doi.org/10.1016/j.epsl.2008.09.030

Reichow, M.K., Saunders, A.D. *et al.* 2016. Petrogenesis and timing of mafic magmatism, South Taimyr, Arctic Siberia: a northerly continuation of the Siberian Traps? *Lithos*, **248–251**, 382–401, https://doi.org/10.1016/j.lithos.2016.01.018

Ritzmann, O., Maercklin, N., Faleide, I.J., Bungum, H., Mooney, W.D. & Detweiler, S.T. 2007. A three-dimensional geophysical model of the crust in the Barents Sea region: model construction and basement characterization. *Geophysical Journal International*, **170**, 417–435, https://doi.org/10.1111/j.1365-246X.2007.03337.x

Roberts, D. 2003. The Scandinavian Caledonides: event chronology, palaeogeographic settings and likely modern analogues. *Tectonophysics*, **365**, 283–299, https://doi.org/10.1016/S0040-1951(03)00026-X

Roberts, D. & Olovyanishnikov, V. 2004. Structural and tectonic development of the Timanide orogen. *In*: Gee, D.G. & Pease, V. (eds) *The Neoproterozoic Timanide Orogen of Eastern Baltica*. Geological Society, London, Memoirs, **30**, 47–57, https://doi.org/10.1144/GSL.MEM.2004.030.01.05

Saltus, R.W., Miller, E.L., Gaina, C. & Brown, P.J. 2011. Regional magnetic domains of the Circum-Arctic: a framework for geodynamic interpretation. *In*: Spencer, A.M., Embry, A.F., Gautier, D.L., Stoupakova, A.V. & Sørensen, K. (eds) *Arctic Petroleum Geology*. Geological Society, London, Memoirs, **35**, 49–60, https://doi.org/10.1144/M35.4

Schaeffer, A.J. & Lebedev, S. 2013. Global shear speed structure of the upper mantle and transition zone. *Geophysical Journal International*, **194**, 417–449, https://doi.org/10.1093/gji/ggt095

Schaeffer, A.J. & Lebedev, S. 2015*a*. Global heterogeneity of the lithosphere and underlying mantle: a seismological appraisal based on multimode surface-wave dispersion analysis, shear-velocity tomography, and tectonic regionalization. *In*: Khan, A. & Deschamps, F. (eds) *The Earth's Heterogeneous Mantle*. Springer Geophysics. Springer International, Switzerland, 3–46.

Schaeffer, A.J. & Lebedev, S. 2015*b*. Seismic tomography of the Arctic lithosphere and asthenosphere. In: *EGU General Assembly Conference Abstracts*, 17, 2819, 12–17 April 2015, Vienna, Austria.

Schaeffer, A.J., Lebedev, S. & Gaina, C. In review. Structure of the Circum-Arctic lithosphere and asthenosphere imaged using multimode waveform tomography. *Tectonophysics*.

Schiffer, C. & Nielsen, S.B. 2016. Implications for anomalous mantle pressure and dynamic topography from lithospheric stress patterns in the North Atlantic Realm. *Journal of Geodynamics*, **98**, 53–69, https://doi.org/10.1016/j.jog.2016.03.014

Schiffer, C. & Stephenson, R.A. In press. Regional crustal architecture of Ellesmere Island, Arctic Canada. *In*: Pease, V. & Coakley, B. (eds) *Circum-Arctic Lithosphere Evolution*. Geological Society, London, Special Publications, **460**, https://doi.org/SP460.8

Schiffer, C., Balling, N., Jacobsen, B.H., Stephenson, R.A. & Nielsen, S.B. 2014. Seismological evidence for a fossil subduction zone in the East Greenland Caledonides. *Geology*, **42**, 311–314, https://dx.doi.org/10.1130/G35244.1

Schiffer, C., Jacobsen, B.H., Balling, N., Ebbing, J. & Nielsen, S.B. 2015*a*. The East Greenland Caledonides – teleseismic signature, gravity and isostasy. *Geophysical Journal International*, **203**, 1400–1418, https://doi.org/10.1093/gji/ggv373

Schiffer, C., Stephenson, R.A., Petersen, K.D., Nielsen, S.B., Jacobsen, B.H., Balling, N. & Macdonald, D.I.M. 2015*b*. A sub-crustal piercing point for North Atlantic reconstructions and tectonic implications. *Geology*, **43**, 1087–1090, https://doi.org/10.1130/G37245.1

Schiffer, C., Stephenson, R., Oakey, G.N. & Jacobsen, B.H. 2016. The crustal structure of Ellesmere Island, Arctic Canada – teleseismic mapping across a remote intraplate orogenic belt. *Geophysical Journal International*, **204**, 1579–1600, https://doi.org/10.1093/gji/ggv539

Senger, K., Tveranger, J., Ogata, K., Braathen, A. & Planke, S. 2014. Late Mesozoic magmatism in Svalbard: a review. *Earth-Science Reviews*, **139**, 123–144, https://doi.org/10.1016/j.earscirev.2014.09.002

Shephard, G.E., Müller, R.D. & Seton, M. 2013. The tectonic evolution of the Arctic since Pangea breakup: integrating constraints from surface geology and geophysics with mantle structure. *Earth-Science Reviews*, **124**, 148–183, https://doi.org/10.1016/j.earscirev.2013.05.012

Sippel, J., Scheck-Wenderoth, M., Lewerenz, B. & Kroeger, K.F. 2013. A crust-scale 3D structural model of the Beaufort–Mackenzie Basin (Arctic Canada). *Tectonophysics*, **591**, 30–51, https://doi.org/10.1016/j.tecto.2012.10.030

Srivastava, S.P. 1985. Evolution of the Eurasian Basin and its implications to the motion of Greenland along

Nares Strait. *Tectonophysics*, **114**, 29–53, https://doi.org/10.1016/0040-1951(85)90006-X

Stein, C.A. & Stein, S. 1992. A model for the global variation in oceanic depth and heat flow with lithospheric age. *Nature*, **359**, 123–129, https://doi.org/10.1038/359123a0

Stemmerik, L., Dalhoff, F., Larsen, B.D., Lyck, J., Mathiesen, A. & Nilsson, I. 1998. Wandel Sea Basin, eastern North Greenland. *Geology of Greenland Survey Bulletin*, **180**, 55–62.

Stephenson, R.A., Boerstoel, J., Embry, A.F. & Ricketts, B.D. 1994*a*. Subsidence analysis and tectonic modelling of the Sverdrup Basin. *In: 1992 Proceedings, International Conference on Arctic Margins*, 2–4 September 1992, Anchorage, AK, USA. US Department of the Interior Minerals Management Service.

Stephenson, R.A., Coflin, K.C., Lane, L.S. & Dietrich, J.R. 1994*b*. Crustal structure and tectonics of the southeastern Beaufort Sea continental margin. *Tectonics*, **13**, 389–400, https://doi.org/10.1029/93TC02251

Stephenson, R., Piepjohn, K., Schiffer, C., von Gosen, W. & Oakey, G.N. In press. Combined crustal-geological cross-section of Ellesmere Island. *In*: Pease, V. & Coakley, B. (eds) *Circum-Arctic Lithosphere Evolution*. Geological Society, London, Special Publications, **460**, https://doi.org/10.1144/SP460.12

Stoupakova, A.V., Henriksen, E. *et al.* 2011. The geological evolution and hydrocarbon potential of the Barents and Kara shelves. *In*: Spencer, A.M., Embry, A.F., Gautier, D.L., Stoupakova, A.V. & Sørensen, K. (eds) *Arctic Petroleum Geology*. Geological Society, London, Memoirs, **35**, 325–344, https://doi.org/10.1144/M35.21

Suckro, S.K., Gohl, K. *et al.* 2012. The crustal structure of southern Baffin Bay: implications from a seismic refraction experiment. *Geophysical Journal International*, **190**, 37–58, https://doi.org/10.1111/j.1365-246X.2012.05477.x

Tegner, C. & Pease, V. 2014. Continental flood basalts of Bennett Island, East Siberian Sea: High Arctic geodynamics. *In*: *EGU General Assembly Conference Abstracts*, 16, 2452, 27 April–2 May 2014, Vienna, Austria.

Tegner, C., Brooks, C.K., Duncan, R.A., Heister, L.E. & Bernstein, S. 2008. $^{40}Ar–^{39}Ar$ ages of intrusions in East Greenland: rift-to-drift transition over the Iceland hotspot. *Lithos*, **101**, 480–500, https://doi.org/10.1016/j.lithos.2007.09.001

Tegner, C., Storey, M., Holm, P.M., Thorarinsson, S.B., Zhao, X., Lo, C.-H. & Knudsen, M.F. 2011. Magmatism and Eurekan deformation in the High Arctic Large Igneous Province: $^{40}Ar–^{39}Ar$ age of Kap Washington Group volcanics, North Greenland. *Earth and Planetary Science Letters*, **303**, 203–214, https://doi.org/10.1016/j.epsl.2010.12.047

Tessensohn, F. & Piepjohn, K. 2000. Eocene compressive deformation in Arctic Canada, North Greenland and Svalbard and its plate tectonic causes. *Polarforschung*, **68**, 121–124.

Thórarinsson, S.B., Holm, P.M., Tappe, S., Heaman, L.M. & Tegner, C. 2011. Late Cretaceous–Palaeocene continental rifting in the High Arctic: U–Pb geochronology of the Kap Washington Group volcanic sequence, North Greenland. *Journal of the Geological Society, London*, **168**, 1093–1106, https://doi.org/10.1144/0016-76492011-018

Thórarinsson, S.B., Holm, P.M., Duprat, H.I. & Tegner, C. 2012. Petrology and Sr–Nd–Pb isotope geochemistry of Late Cretaceous continental rift ignimbrites, Kap Washington peninsula, North Greenland. *Journal of Volcanology and Geothermal Research*, **219–220**, 63–86, https://doi.org/10.1016/j.jvolgeores.2012.01.011

Thórarinsson, S.B., Söderlund, U., Døssing, A., Holm, P.M., Ernst, R.E. & Tegner, C. 2015. Rift magmatism on the Eurasia basin margin: U–Pb baddeleyite ages of alkaline dyke swarms in North Greenland. *Journal of the Geological Society, London*, **172, 721–726**, https://doi.org/10.1144/jgs2015-049

Tomurtogoo, O., Windley, B.F., Kröner, A., Badarch, G. & Liu, D.Y. 2005. Zircon age and occurrence of the Adaatsag ophiolite and Muron shear zone, central Mongolia: constraints on the evolution of the Mongol–Okhotsk ocean, suture and orogen. *Journal of the Geological Society, London*, **162**, 125–134, https://doi.org/10.1144/0016-764903-146

Torsvik, T.H. & Andersen, T.B. 2002. The Taimyr fold belt, Arctic Siberia: timing of prefold remagnetisation and regional tectonics. *Tectonophysics*, **352**, 335–348, https://doi.org/10.1016/S0040-1951(02)00274-3

Trettin, H.P. 1987. Pearya: a composite terrane with Caledonian affinities in northern Ellesmere Island. *Canadian Journal of Earth Sciences*, **24**, 224–245, https://doi.org/10.1139/e87-025

Trettin, H.P. 1991*a*. Silurian–early Carboniferous deformational phases and associated metamorphism and plutonism, Arctic Island. *In*: Trettin, H.P. (ed.) *Geology of the Innuitian Orogen and Arctic Platform of Canada and Greenland*. Geological Survey of Canada, Geology of Canada, **3**, 295–341.

Trettin, H.P. 1991*b*. Tectonic framework. *In*: Trettin, H.P. (ed.) *Geology of the Innuitian Orogen and Arctic Platform of Canada and Greenland*. Geological Survey of Canada, Geology of Canada, **3**, 57–66.

Trettin, H.P. & Parrish, R. 1987. Late Cretaceous bimodal magmatism, northern Ellesmere Island: isotopic age and origin. *Canadian Journal of Earth Sciences*, **24**, 257–265, https://doi.org/10.1139/e87-027

Van Wagoner, N.A., Williamson, M.-C., Robinson, P.T. & Gibson, I.L. 1986. First samples of acoustic basement recovered from the alpha ridge, Arctic ocean: new constraints for the origin of the ridge. *Journal of Geodynamics*, **6**, 177–196, https://doi.org/10.1016/0264-3707(86)90038-4

Van Wijk, J.W. & Blackman, D.K. 2005. Dynamics of continental rift propagation: the end-member modes. *Earth and Planetary Science Letters*, **229**, 247–258, https://doi.org/10.1016/j.epsl.2004.10.039

Vol'nov, D.A. & Sorokov, D.S. 1961. The geology of the Bennett Island. *In*: Tkachenko, B.V. (ed.) *Sb. statei po geologii i neftegazonosnosti Arktiki* (Collection of Research Papers on the Geology and Oil and Gas Resources of the Arctic), Leningrad, **123**, 5–18.

WALDERHAUG, H.J., EIDE, E.A., SCOTT, R.A., INGER, S. & GOLIONKO, E.G. 2005. Palaeomagnetism and $^{40}Ar/^{39}Ar$ geochronology from the South Taimyr igneous complex, Arctic Russia: a Middle–Late Triassic magmatic pulse after Siberian flood-basalt volcanism. *Geophysical Journal International*, **163**, 501–517, https://doi.org/10.1111/j.1365-246X.2005. 02741.x

WANG, Z. & DAHLEN, F.A. 1995. Spherical-spline parameterization of three-dimensional earth models. *Geophysical Research Letters*, **22**, 3099–3102, https://doi.org/10.1029/95GL03080

ZHANG, X., OMMA, J., PEASE, V. & SCOTT, R. 2013. Provenance of Late Paleozoic–Mesozoic sandstones, Taimyr Peninsula, the Arctic. *Geosciences*, **3**, 502–527, https://doi.org/10.3390/geosciences3030502

ZHANG, X., PEASE, V., SKOGSEID, J. & WOHLGEMUTH-UEBERWASSER, C. 2015. Reconstruction of tectonic events on the northern Eurasia margin of the Arctic from U–Pb detrital zircon provenance investigations of late Paleozoic to Mesozoic sandstones in southern Taimyr Peninsula. *Geological Society of America Bulletin*, B31241.1, https://doi.org/10.1130/B31241.1

ZHANG, X., PEASE, V., CARTER, A., KOSTUYCHENKO, S., SULEYMANOV, A. & SCOTT, R. In press *a*. Timing of exhumation and deformation across the Taimyr fold and thrust belt: Insight from apatite fission track dating and balanced cross-sections. *In*: PEASE, V. & COAKLEY, B. (eds) *Circum-Arctic Lithosphere Evolution*. Geological Society, London, Special Publications, **460**, https://doi.org/SP460.3

ZHANG, X., PEASE, V., CARTER, A. & SCOTT, R. In press *b*. Reconstructing Palaeozoic & Mesozoic Tectonic Evolution of Novaya Zemlya: Combing Geochronology and Thermochronology. *In*: PEASE, V. & COAKLEY, B. (eds) *Circum-Arctic Lithosphere Evolution*. Geological Society, London, Special Publications, **460**, https://doi.org/10.1144/SP460.13

ZIENKIEWICZ, O.C. 1977. *The Finite Element Method*. McGraw-Hill, Maidenhead.

ZORIN, Y.A. 1999. Geodynamics of the western part of the Mongolia–Okhotsk collisional belt, Trans-Baikal region (Russia) and Mongolia. *Tectonophysics*, **306**, 33–56, https://doi.org/10.1016/S0040-1951(99)00042-6